Arctic shelves as platforms for biogeochemical activity: nitrogen and carbon transformations in the Chukchi Sea, Alaska

Amber K. Hardison[1*]

amber.hardison@utexas.edu

Nathan D. McTigue[1,2]

nathan.mctigue@noaa.gov

Wayne S. Gardner[1]

wayne.gardner@utexas.edu

Kenneth H. Dunton[1]

ken.dunton@utexas.edu

[1]University of Texas at Austin Marine Science Institute, 750 Channel View Drive, Port Aransas, TX, 78373, USA

[2]NOAA Center for Coastal Fisheries and Habitat Research, Beaufort, NC 28516, USA

*Corresponding author

Abstract

Continental shelves comprise <5% of global ocean area but may account for a disproportionate 30% of primary production, 80% of organic matter burial, and >50% of marine denitrification. The Hanna Shoal region, part of the continental shelf system in the northeast Chukchi Sea, Alaska, is recognized for its high biodiversity and productivity. We investigated the role of sediments in organic matter decomposition and nutrient cycling at five stations on the shallow Hanna Shoal. In particular, we asked (1) how much sediment organic matter is remineralized in the Chukchi Sea, and what factors drive this degradation, (2) do sediments function as a net source for fixed nitrogen (thus fueling primary production in the overlying water), or as a net sink for fixed nitrogen (thereby removing it from the system), and (3) what is the balance between sediment NH_4^+ uptake and regeneration, and what factors drive NH_4^+ cycling? We conducted dark sediment core incubations to measure sediment O_2 consumption, net N_2 and nutrient (NH_4^+, NO_3^-, NO_2^-, PO_4^{3-}) fluxes, and rates of sediment NH_4^+ cycling, including uptake and regeneration. Rates of sediment O_2 consumption and NH_4^+ and PO_4^{3-} efflux suggest that high organic matter remineralization rates occurred in these cold (-2 °C) sediments. We estimated that total organic carbon remineralization accounted for 20 – 57% of summer export production measured on the Chukchi Shelf. Net N_2 release was the dominant nitrogen flux, indicating that sediments acted as a net sink for bioavailable nitrogen via denitrification. Organic carbon remineralization via denitrification accounted for 6 – 12% of summer export production, which made up ~25% of the total organic carbon oxidized in Hanna Shoal sediments. These shallow, productive Arctic shelves are “hotspots” for organic matter remineralization.

KEYWORDS: Chukchi Sea, sediments, nitrogen cycle, denitrification, organic carbon mineralization

1. Introduction

The majority of global marine primary production occurs on continental shelves, as their high nutrient levels and shallow nature make them "hotspots" for organic matter production and export (Bauer et al., 2013; Smith and Hollibaugh, 1993). The Arctic contains ~20% of the world's continental shelves even though it represents only 4% of the global ocean area, and this region is recognized for high rates of primary production during the ice-free growing season (Arrigo and van Dijken, 2011; Grebmeier et al., 2006; Sørensen et al., 2015). The Chukchi Sea is a dynamic region within the Arctic through which upwelled, nutrient-rich Pacific Ocean water flows from the Bering Strait towards the Arctic Ocean basin. The high nutrient levels support high levels of primary production over the broad northern Chukchi Sea shelf, averaging 80-90 g C m^{-2} y^{-1} (Codispoti et al., 2013). Low levels of grazing and remineralization in the shallow water column there lead to high rates of export production to the benthos, which fuels a productive benthic faunal community, promotes a tightly coupled food web, and supports high sediment decomposition (Chang and Devol, 2009; Dunton et al., 1989; Grebmeier et al., 2015; Moran et al., 2005).

Sediments are critical zones of organic matter cycling, including recycling and removal of carbon and nutrients. Organic matter remineralization occurs via oxidative reactions in which the terminal electron acceptors are O_2, NO_3^-, Mn-oxides, Fe-oxides, SO_4^{2-}, and CO_2. The relative importance of these different pathways changes with sediment type and sedimentation rates (Canfield et al., 1993). Most of the reduced species produced by anaerobic remineralization are ultimately re-oxidized by an equivalent amount of O_2. Thus, O_2 uptake is often used as a proxy for total benthic organic carbon remineralization, which is the sum of oxic and anoxic

remineralization. Total O_2 uptake (TOU) can be split into (1) diffusive O_2 uptake (DOU), due to aerobic respiration by benthic microbes, and (2) advective O_2 uptake, generally governed by benthic faunal activities. TOU can be measured using benthic chambers settled on the seafloor (e.g., Reimers et al., 2001) or, as in the current study, ex situ using sediment core incubations (Archer and Devol, 1992; Arrigo and van Dijken, 2011). DOU is quantified by the use of microelectrodes performed in situ or ex situ with sediment cores (Arrigo and van Dijken, 2011; Glud et al., 1994).

Remineralization of organic matter produces dissolved inorganic compounds (e.g., CO_2, NH_4^+, NO_3^-, PO_4^{3-}), which can be released to the overlying water and may fuel further pelagic productivity. In some systems, sediment nutrient release satisfies a large proportion of the inorganic nitrogen and phosphorus requirements for pelagic primary production (Joye and Anderson, 2008; Nixon, 1981). This "internal" loading of nutrients, particularly nitrogen, may be important in the Chukchi Sea, as previous work suggests that nitrogen is the limiting macronutrient over the Chukchi shelf (Brown et al., 2015; Gruber and Sarmiento, 1997; Risgaard-Petersen, 2004). While the ultimate source of bioavailable nitrogen in the Chukchi Sea is northward flow through the Bering Strait, local regeneration from organic-rich shallow sediments may supply a large fraction of available nitrogen seasonally. Sediments also play an important role in nitrogen loss. The processes of denitrification and anammox, which occur in anoxic sediments, completely remove fixed nitrogen from a system via N_2 gas, which is unavailable to most organisms. Heterotrophic denitrification is the major removal pathway of bioavailable nitrogen in the ocean (Devol, 2015; Nixon, 1981). Understanding the role of sediments in the fate of organic matter is critical to ecosystem functioning in continental shelf

systems. Specifically, the dominant nitrogen cycling pathway occurring in sediments will determine whether sediments act as a net source or a sink for fixed nitrogen.

Few studies of sediment organic carbon remineralization and nitrogen cycling have been conducted in the Pacific Arctic due largely to the logistical difficulties of studying the region, which is ice-covered for the majority of the year. Sediment O_2 fluxes have been studied in the Chukchi Sea relatively recently (see Grebmeier et al. 2006 review). Sediment nitrogen cycling, including ammonification and denitrification are studied less frequently (Chang and Devol, 2009; Devol et al., 1997; McTigue et al., 2016; Rowe and Phoel, 1992; Souza et al., 2014b), and benthic O_2 fluxes and nitrogen cycling have been studied together only three times in the Chukchi Sea (Christensen et al., 1987; Souza et al., 2014; McTigue et al., 2016). Approximately 20-22% of primary production is remineralized in Chukchi Sea shelf sediments, which in turn is influenced by a range of environmental factors, including water column depth and integrated chlorophyll *a*, sediment organic carbon, and infaunal biomass (Grebmeier 2006; Moran et al. 2005). Arctic shelves may contribute a significant 4-13% of the total sink of fixed nitrogen in the global ocean via denitrification, which is influenced by cumulative organic matter deposition on the seafloor (Chang and Devol, 2009). These and studies in other areas of the Arctic (e.g., Glud et al., 1998; Rysgaard et al., 2004; Sørensen et al., 2015) suggest that Arctic sediments are dynamic zones of organic matter remineralization that vary over space and time; however, additional studies in the Chukchi Sea would further capture this variability.

This study focuses on the Hanna Shoal, a highly productive region of the northern Chukchi shelf. Hanna Shoal is unique in that it has extremely high production and particle flux due to hydrodynamic forcings that focus export production to the seafloor (Carini et al., 2010; Grebmeier et al., 2015; Schonberg et al., 2014). It has notably high benthic fauna, marine

mammals, and birds, due to its shallow nature and the presence of ice during the summer, which make it easy to access for feeding (Schonberg et al., 2014). Information is limited about the role of sediments in the fate of this organic matter, including carbon and nutrient recycling and removal. We measured simultaneous fluxes of O_2, N_2, and dissolved inorganic nutrients at the sediment-water interface in the Hanna Shoal region in summer 2013. This research is guided by the following questions and hypotheses: (1) How much sediment organic matter is remineralized in the Chukchi Sea, and what factors drive this degradation? We hypothesize that highest organic matter remineralization rates will correspond to highest sediment organic content. (2) Are the sediments a net sink or source of fixed nitrogen? We hypothesize that sediments are a net sink for fixed nitrogen via denitrification because they provide suitable biogeochemical conditions (high quality organic matter) at the sediment surface, which provides energy for heterotrophic denitrification. (3) What is the balance between sediment NH_4^+ uptake and regeneration, and what factors drive NH_4^+ cycling? We hypothesize that the highest rates of NH_4^+ uptake and regeneration will take place at stations with higher sediment organic content. We examine biogeochemical transformation of organic matter at the sediment-water interface in the Hanna Shoal ecosystem to address these questions and hypotheses and improve understanding of how sediments influence system-wide productivity and nitrogen cycling.

2. Materials and methods

2.1 Study sites and sampling

The study was conducted on board the USCGC *Healy* in the northeastern Chukchi Sea, Alaska from July to August 2013 as part of the Hanna Shoal Ecosystem Study (*http://arcticstudies.org/hannashoal/*). The Hanna Shoal is a bathymetric feature of the Chukchi Sea, but the area surrounding it is a known biological hotspot. Five stations (41 – 66 m depth) were sampled across the Hanna Shoal region for biogeochemical rate determination (Fig. 1). At each station, bottom water samples (40 L) for incubations were collected by CTD cast, and six sediment cores (7.6 cm I.D. x 20 cm length) with intact sediment-water interfaces were collected using a HYPOX corer (Gardner et al., 2009) with a stainless steel lander. Sediments and water were stored in an environmental chamber at 4 °C. At each station, bottom water temperature, salinity, and dissolved O_2 concentration were recorded with a CTD. Additional sediments were collected via van Veen grab (0.1 m^2) for organic matter and chlorophyll content. Samples for elemental carbon and nitrogen and pigment analyses were collected from the top 2 cm of sediment with a 10 mL syringe barrel and immediately frozen at -20 °C.

2.2 Oxygen microprofiles

At each station, three to five O_2 microprofiles were measured in two of the intact cores using Clark-type O_2 microelectrodes (OX-50, Unisense). O_2 measurements were made in vertical steps of 500 μm in the dark at 4 °C with gentle stirring of the overlying water, which was kept at near bottom water concentrations. Generally, profiles were measured in areas unaffected by faunal activity. Oxygen penetration depth (OPD) and diffusive O_2 fluxes (diffusive O_2 utilization, DOU) were determined by applying a classical steady-state one-dimension diffusion-reaction model (Boudreau, 1997; Soetaert and Meysman, 2009; Brin et al. 2014):

$$\varphi(DO_2/\theta^2)(d^2O_2/dt^2) = v_{max}(O_2)/(O_2 + kO_2) \quad (1)$$

where φ is the sediment porosity (0-1 cm) and is constant for each site, DO_2 is the temperature- and salinity-corrected diffusion coefficient for O_2, θ^2 is the tortuosity determined by $\theta^2 = (1 - \ln(\varphi^2))$ (Boudreau 1997), and v_{max} and kO_2 are Monod-type kinetic parameters describing sediment O_2 consumption. R (www.r-project.org; R Development Core Team 2013) was used to set up the model using the reactive transport (Soetaert and Meysman 2009) and flexible modeling environment (Soetaert and Petzoldt 2012) packages. Sediment porosity values were obtained for each station from J. Trefry (unpublished).

2.3 Measuring solute fluxes at the sediment-water interface

The four remaining cores per station were incubated in the environmental chamber at 4 °C. Cores were connected to a flow-through incubation system as described by McTigue et al. (2016), and based on Gardner and McCarthy (2009). Briefly, an air-tight cap was placed in each core, leaving ~230 mL of water overlying the sediments. Aerated, unfiltered site bottom water was pumped continuously through inflow tubing, over the sediment-water interface, then through outflow tubing at ~1.2 mL min^{-1}. The inflow bottom water was divided into two treatments: (1) unamended, control water to measure net N_2, O_2, and nutrient fluxes, and (2) spiked with ^{15}N-NH_4^+ (99.9% ^{15}N-NH_4Cl) to final concentrations between 15-18 μM NH_4^+, depending on ambient NH_4^+ concentrations (Table 1), to measure NH_4^+ cycling rates. Each feed water reservoir fed duplicate cores, and cores were wrapped in aluminum foil to ensure dark conditions.

After an initial 12 h pre-incubation to allow the flow-through system to reach equilibrium, inflow and outflow water were sampled for dissolved gas and nutrient

concentrations once daily for four days. Samples for dissolved gases (O_2, N_2) were collected from the control cores in 13 mL Exetainers (Labco, UK) by allowing the vials to overflow three times, ensuring no air bubbles were captured. Each sample was killed with 200 μL of saturated $ZnCl_2$, capped, and stored submerged at 4 °C. Samples were collected from the control cores for dissolved nutrient concentrations. 30 mL of water was passed through a 0.2 μm filter into a Whirlpak bag and frozen until analysis. All water samples were collected in duplicate for analytical replication. Samples were transported to the University of Texas Marine Science Institute (UTMSI) for analyses.

Dissolved gas concentrations (O_2, N_2, and Ar) were measured using membrane inlet mass spectrometry (MIMS) (Kana et al., 1994). Water and CO_2 from the gas sample were cryogenically trapped in-line prior to gases entering the mass spectrometer. Analytical replicates (n = 3) for dissolved gases had a coefficient of variation < 0.04%. Air-saturated (100%) ultraclean deionized water was used as a standard. Samples for NO_3^-, NO_2^-, NH_4^+, and PO_4^{3-} concentrations were prepared using standard colorimetric techniques adapted to a microplate spectrophotometer (Mooney and McClelland, 2012), as described previously in McTigue et al. (2016). Precision (SE) of NO_3^- + NO_2^- concentrations was 6%, NH_4^+ was 4%, and PO_4^{3-} was 4% (Mooney and McClelland, 2012).

Benthic fluxes of dissolved constituents (μmol m^{-2} h^{-1}) were calculated as the difference between outflow and inflow concentrations at the same time point:

$$flux = (C_o - C_i) \times \frac{\mathrm{F}}{A} \quad (2)$$

where C_o and C_i are the outflow and inflow concentrations, respectively (μM), F is the flow rate (L h^{-1}), and A is the sediment cross-sectional area (m^2) (Lavrentyev et al., 2000). A positive flux indicates release from the sediments to the overlying water, or efflux, while a negative flux designates uptake by the sediments, which we also refer to as influx, consumption, or demand. Specifically, a negative O_2 flux corresponds to sediment O_2 demand, or total O_2 utilization (TOU). A positive N_2 flux corresponds to net denitrification, while a negative N_2 flux indicates net nitrogen fixation.

2.4 Measuring NH_4^+ cycling rates at the sediment-water interface

Since net NH_4^+ flux across the sediment-water interface is the sum of simultaneous NH_4^+ uptake and regeneration, sediment NH_4^+ uptake and regeneration rates were determined in the $^{15}NH_4^+$ core incubations according to Lin and colleagues (2011). Duplicate inflow and outflow water samples were collected as described above for nutrient analyses. NH_4^+ isotopic composition was measured at UTMSI using ammonium isotope retention time shift (AIRTS) high-performance liquid chromatography (HPLC; Gardner, 1995). Each sample was run in triplicate, and an internal NH_4^+ standard was included between samples (CV < 5%).

NH_4^+ regeneration and uptake rates were calculated according to the isotope dilution equations developed by Blackburn (1979) and modified by Lin et al. (2011) for the flow-through incubation technique. The calculations require the relative abundance of $^{15}NH_4^+$ in the total NH_4^+ pool, as follows:

$$r = {}^{15}NH_4^+ / ({}^{15}NH_4^+ + {}^{14}NH_4^+). \quad (3)$$

The actual NH_4^+ regeneration (*REG*) and potential uptake (U_{pot}) rates are calculated as:

$$REG = \frac{\ln(\frac{r_i}{r_o})}{\ln(\frac{C_o}{C_i})} \times (C_o - C_i) \times \frac{F}{A} \quad (4)$$

$$U_{pot} = \left(1 - \frac{\ln\left(\frac{r_i}{r_o}\right)}{\ln\left(\frac{C_o}{C_i}\right)}\right) \times (C_o - C_i) \times \frac{F}{A}$$

(5)

where rates are in μmol m^{-2} h^{-1}; r_i and r_o are the inflow and outflow isotope ratios of $^{15}NH_4^+$ in the $^{15}NH_4^+$ treatments, respectively; and C_i and C_o are the inflow and outflow NH_4^+ concentrations in the $^{15}NH_4^+$ treatments, respectively (μM). Regeneration is expressed as a positive flux. The potential uptake rate (expressed as a negative flux) includes consumption via nitrification, assimilation, and other NH_4^+ removal processes (Lin et al., 2011).

The net flux of NH_4^+ across the sediment-water interface at each site is estimated using the net NH_4^+ flux from the control cores. We assume that the $^{15}NH_4^+$ addition and control cores have the same NH_4^+ regeneration fluxes because the added $^{15}NH_4^+$ is the end product rather than the substrate of regeneration. Based on this assumption, the actual uptake flux (U_{act}) is defined as the net NH_4^+ flux from the control cores (*NET*) minus the actual NH_4^+ regeneration rate in the $^{15}NH_4^+$ cores (*REG*):

$$U_{act} = NET - REG \quad (6)$$

where U_{act} rates (expressed as a negative flux) are in μmol m^{-2} h^{-1}. The difference between potential and actual uptake can be described as "Sediment NH_4^+ Demand" (SAD; expressed as a positive value), which reflects the degree of NH_4^+ limitation on the microbial community:

$$SAD = U_{pot} - U_{act} \quad (7)$$

As the difference between potential and actual uptake decreases, addition of NH_4^+ is less likely to stimulate microbial activity, and SAD decreases.

2.5 Sediment characterization

Sediment samples for total organic carbon and total nitrogen were soaked in 1 N HCl until bubbling stopped to remove carbonates, then rinsed in deionized water and dried at 60 °C. Sediments were homogenized and analyzed on an elemental analyzer (CE Instruments, NC 2500). Samples for chlorophyll *a* content were processed according to McTigue et al. (2015). Briefly, chlorophyll *a* was extracted with 10 mL of acetone in the dark in chilled water using sonication. Samples were centrifuged for 5 min. at 4000 rpm, and the supernatant was filtered through 0.2 μm nylon filters. Each sample was extracted twice, and the extracts were combined. Filtrate was analyzed via HPLC, and chlorophyll *a* concentration was determined by comparing the pigment peak to those of a certified commercial standard.

2.6 Statistical analyses

All statistics were computed using R. For all rates, the mean value for each core was obtained by averaging the daily measurements (T_0, T_1, T_2, T_3; n = 4). Repeated measures ANOVA was performed to ensure that cores had reached steady-state conditions by the first sampling. The results underwent post-hoc testing using Tukey's comparisons, and significantly different rates at T_0 or T_1 were omitted. The mean value for each treatment (control or $^{15}NH_4^+$) was obtained by averaging the duplicate core means (n = 2). Stations were compared using a 1-way ANOVA. The results underwent post-hoc testing using Tukey's comparisons. A Pearson correlation matrix was created using mean rates and environmental parameters from each station. For all tests, alpha = 0.05.

3. Results

3.1 Site characteristics

The five stations spanned a region approximately 250 km x 100 km (Fig. 1). The stations were alike in many aspects: water depths ranged from 41 to 66 m, bottom water temperature (mean -1.6 ± 0.02 ºC), salinity (mean 32.7 ± 0.02), dissolved O_2 (mean 79 ± 2%) and nutrient data were comparable, and surface sediment organic content (TOC mean 1.2 ± 0.2 %; TN mean 0.2 ± 0.03 %) was similar (see Table 1 for selected and McTigue et al., 2016, for full site metadata). Moderate sediment organic content corresponded to moderately shallow OPDs, which ranged from 5.5 ± 0.5 mm at CBL13 to 7.6 ± 0.2 mm at H29 (Table 1). Benthic chlorophyll *a* concentrations ranged from 8.3 (H29) to 35.2 mg m^{-2} (CBL13; Table 1).

3.2 Net dissolved gas and nutrient fluxes

Diffusive O_2 uptake (DOU) rates obtained from O_2 microprofiles ranged from -139 ± 43 to -222 ± 33 μmol O_2 m^{-2} h^{-1} at CBL11 and CBL13, respectively (Fig. 2a; Table 2). The average DOU rate across stations was -179 ± 15 μmol O_2 m^{-2} h^{-1}. Whole core dissolved gas fluxes from incubations are unavailable for station H17 due to instrument malfunction. Net O_2 fluxes, or total O_2 uptake (TOU) at the remaining 4 stations were all directed into the sediments, indicating net O_2 consumption by sediment organisms. O_2 fluxes ranged from -157 ± 11 to -452 ± 166 μmol O_2 m^{-2} h^{-1} at CBL13 and H33, respectively, with significantly higher O_2 consumption at H33 (Fig. 2a; Table 2). The station averaged TOU rate (-266 ± 68 μmol O_2 m^{-2} h^{-1}) was greater (more negative) than the DOU rate. Net N_2 fluxes were directed out of the sediments at all stations, indicating net N_2 production via denitrification or anammox (Fig. 2b; Table 2). Values ranged from 24 ± 4 (H29) to 55 ± 3 μmol N m^{-2} h^{-1} (CBL11) and were highest at CBL11. Net N_2 flux averaged across stations was 38 ± 7 μmol N m^{-2} h^{-1}.

Net NH_4^+ and PO_4^{3-} fluxes were directed out of the sediments for most stations, and NH_4^+ fluxes always exceeded PO_4^{3-} fluxes (Fig. 2c, 2d; Table 2). Net NH_4^+ fluxes ranged from -0.1 ± 4.3 (H17) to 10.7 ± 3.6 μmol NH_4^+ m^{-2} h^{-1} (CBL13) and were not significantly different among stations. Net PO_4^{3-} fluxes ranged from -0.5 ± 0.5 (H17) to 3.3 ± 1.2 μmol PO_4^{3-} m^{-2} h^{-1} (H29). PO_4^{3-} fluxes at station H29 and H17 were significantly different from each other, but not from the other stations. NH_4^+ and PO_4^{3-} fluxes at H17 were not significantly different from zero, indicating no net release or uptake by sediments (within the detection limits of the methods). In contrast to NH_4^+ and PO_4^{3-}, net NO_3^- fluxes at all stations were negative, indicating uptake into sediments, and all stations were not statistically different from one another (Fig. 2e; Table 2).

Values ranged from -3.8 ± 0.9 (H29) to -23.5 ± 7.5 μmol NO_3^- m^{-2} h^{-1} (H33). Net NO_2^- fluxes were not significantly different from zero at H29 and H33, indicating no net NO_2^- flux into or out of these sediments (Fig. 2f; Table 2). CBL 11 and H17 were significantly different from one another but not from the other stations. CBL11 showed a small net NO_2^- efflux while H17 showed a small net NO_2^- influx.

3.3 NH_4^+ cycling

Although net NH_4^+ fluxes were zero at H17 and showed net release at the other stations (Fig. 2c), the $^{15}NH_4^+$ addition treatment allowed a more detailed analysis of NH_4^+ cycling at the sediment-water interface (Lin et al., 2011). Actual NH_4^+ regeneration rates ranged from 5 ± 2 to 15 ± 2 μmol N m^{-2} h^{-1} with lowest rates at H29 and highest rates at CBL11 (Fig. 3a; Table 3). Station averaged NH_4^+ regeneration was 10.5 ± 1.0 μmol N m^{-2} h^{-1}. Potential uptake rates, measured after $^{15}NH_4^+$ addition, were highest at CBL11 and lowest at H33, ranging from -16 ± 13 to -48 ± 20 μmol N m^{-2} h^{-1} (Fig. 3b; Table 3), with a station average of -35.7 ± 5.4 μmol N m^{-2} h^{-1}. Actual uptake rates at CBL13 were positive, indicating no uptake, while rates ranged from -1.6 ± 1.6 to -17 ± 9 μmol N m^{-2} h^{-1} at the other four stations, with highest actual uptake rates measured at H17 (Fig. 3c; Table 3). Actual uptake rates averaged across stations was -5.7 ± 4 μmol N m^{-2} h^{-1}. The differences between actual and potential uptake rates across stations resulted in similar sediment NH_4^+ demand (SAD) at stations CBL11, CBL13, and H29 (range 36 ± 22 to 46 ± 20 μmol N m^{-2} h^{-1}) while stations H17 and H33 were not significantly different from zero (Fig. 3d; Table 3). The SAD station average was 29.6 ± 6.6 μmol N m^{-2} h^{-1}. All NH_4^+ cycling rates were not significantly different among stations.

3.4 Controls on rates

Correlation analyses reveal several potential environmental controls on measured rates (Table 4). TOU (expressed as a negative value) in Hanna Shoal sediments was correlated positively with sediment TOC and TN content (Table 4; Fig.4). DOU (expressed as a negative value) showed a positive correlation with N_2 and a negative, though not significant, correlation with sediment organic content, thus the highest (most negative) DOU rates occurred at stations with lowest N_2 flux and highest sediment organic content (Fig. 4). N_2 flux was correlated negatively with depth, TOC, TN, TOU, and DOU (Fig. 4; Table 4). NH_4^+ flux correlated positively with benthic chlorophyll *a* concentrations, while dissolved PO_4^{3-} was correlated positively with depth. Regeneration rates were correlated negatively with TOU and correlated positively with DOU. Actual uptake (expressed as a negative value) was correlated negatively with bottom water dissolved O_2 concentrations and correlated positively with sediment TOC, TN, and benthic chlorophyll *a*. Potential uptake and SAD did not correlate with any of the measured environmental controls.

4. Discussion

4.1 Active organic matter remineralization at perennially cold sites in the Chukchi Sea

4.1.1 Sediment O_2 consumption

Sediment O_2 consumption is often used to assess benthic organic matter remineralization (Arrigo and van Dijken, 2011; Glud et al., 2008). All O_2 microprofiles in this study showed rapid consumption of O_2 within a few mm of the sediment-water interface, indicating the high reactivity of these surficial sediments. The OPD into sediments reflects the balance between downward diffusive transport of O_2 from the overlying water and O_2 consumption processes in the sediments. OPD ranged from 5.5 to 7.5 mm, displaying little variability among stations. The DOU rates, which are calculated based on the O_2 profiles, varied only by ~8% across stations. TOU rates, measured in the core incubations, were more variable (CV = 25%). Absolute values were highest at H33 and lowest at CBL13. The ratio of TOU to DOU reflects the degree of macrofaunal irrigation and respiration activities, with higher values corresponding to more macrofaunal activity (Wenzhofer and Glud, 2002). TOU:DOU ratios ranged from 2.9 ± 1.2 to 0.7 ± 0.1 (Table 2). Since TOU:DOU cannot theoretically be less than 1.0, we attribute the two stations with ratios < 1.0 (CBL13 and H29) to variability of the two O_2 flux methods (Table 2). We view these stations to have TOU = DOU. Macrofaunal bioirrigation contributed more to enhancement of the total O_2 flux at H33 and CBL11 than at H29 and CBL13. H33 and CBL11 were dominated by bivalves while CBL13 and H29 were dominated by polychaetes (McTigue et al., 2016), which may exert different influence on sediment O_2 exchange (e.g., Glud et al., 1994; Michaud et al., 2005). Organic matter mineralization due to sediment bacteria, represented by DOU, varied little across stations, perhaps due to the relatively similar environmental conditions (e.g., bottom water temperature and dissolved O_2, which may influence DOU) among stations. DOU measured by O_2 microprofiling may underestimate actual bacterial respiration because it excludes bacterial O_2 consumption in burrows and funnels of any infauna present (Glud 2008).

Although this contribution is captured in the TOU fluxes, our bacterial O_2 consumption estimates based on DOU are conservative.

Our O_2 fluxes were within the range of results from other studies at similar depths in the Chukchi. For example, Grebmeier and colleagues (2006) reviewed patterns of organic carbon production, export, and use in the northern Bering and Chukchi Seas. They reported sediment community oxygen consumption (SCOC, equivalent to TOU) in the northern Chukchi shelf at depths of 50 – 200 m of -125 to -1,667 μmol O_2 m^{-2} h^{-1}. Their highest absolute rates, roughly three times higher than our average rates, were measured in the Barrow Canyon region, where very high rates of primary production and benthic infaunal biomass occur (Table 5; Fig. 5). SCOC rates were correlated to integrated water column chlorophyll *a* concentration, benthic biomass and depth, showing evidence for tight benthic-pelagic coupling in the Chukchi. Stations in the southern and northern Chukchi shelf at depths of 34 – 46 m had a sediment O_2 demand of -150 to -569 μmol O_2 m^{-2} h^{-1} (Souza et al. 2014b) which are nearly identical to those measured in the current study (Table 5; Fig. 5).

Our TOU rates in the Chukchi are also similar to those measured in shelf regions of Norway and Greenland, other Arctic regions with similar temperatures, depth, light levels, and a short burst of primary production during the ice-free season as the Chukchi and Beaufort Seas (Table 5; Fig. 5). One study had absolute TOU rates that were higher than ours (-150 to -845 μmol O_2 m^{-2} h^{-1}), however those rates were measured at a shallower coastal station with higher sediment organic content than our study (Glud et al. 2000).

4.1.2 Sediment nutrient fluxes

In addition to consuming O_2, benthic organic matter remineralization often results in production and release of NH_4^+ and PO_4^{3-} from the sediments to the overlying water, which may fuel water column production. We observed sediment release of NH_4^+ and PO_4^{3-} at all stations except H17, where fluxes were not significantly different from zero. This may be due to lower amounts and/or composition differences of sediment organic content at H17 (Table 1), which may have limited remineralization rates. At the other stations, NH_4^+ and PO_4^{3-} fluxes were variable within and between stations, but did not relate to measured environmental variables, except that PO_4^{3-} was correlated positively with depth (Table 4). NH_4^+ may be released through processes other than ammonification, including dissimilatory NO_3^- reduction to NH_4^+ (DNRA) and faunal excretion. Our companion study at these stations using ^{15}N tracers detected DNRA but the rates were low (McTigue et al. 2016), thus most NH_4^+ release from these sediments likely resulted from ammonification or faunal excretion. The elevated NH_4^+ release at CBL13 may have resulted from the high abundance of infauna there (6,713 ± 678 inv. m^{-2}) relative to the other stations, as described by McTigue et al. (2016). Infauna abundance at CBL13 was dominated by *Maldane sarsi*, a tube-building polychaete, which can enhance sediment NH_4^+ fluxes through excretion and NH_4^+ regeneration via stimulation of bacterial remineralization (Braeckman et al., 2014; Christensen et al., 2000). In contrast to NH_4^+ and PO_4^{3-}, all NO_3^- and most NO_2^- fluxes were directed into the sediments, with NO_3^- values exceeding NO_2^-. This substantial NO_x ($NO_2^- + NO_3^-$) influx may indicate direct denitrification of NO_3^- from overlying water, as discussed below. At stations CBL11 and CBL13, NH_4^+ efflux was greater than NO_x uptake, while at stations H17, H29, and H33, NO_x uptake rates were greater, yielding net DIN ($NO_x + NH_4^+$) fluxes ranging from -14.8 ± 8.8 to 1.5 ± 4.0 μmol N m^{-2} h^{-1} (Table 2). Although NH_4^+ was released from sediments at nearly all stations, sediments at Hanna Shoal were actually

a small net sink for DIN, taking up 3.7 ± 3.1 μmol N m^{-2} h^{-1} when averaged across stations, due to the substantial NO_x influx (Fig. 6). NO_x fluxes did not correlate with any of the measured environmental controls (Table 4).

The few previous nutrient flux studies in this region support our results. Significant fluxes of NH_4^+ from Chukchi shelf sediments provided evidence of local nitrogen regeneration in sediments (Brown et al., 2015; Devol et al., 1997; Henriksen et al., 1993). Likewise, studies in other Arctic regions show NH_4^+ efflux within the range of our rates (Table 5). However, regional or temporal differences exist, as a study in the Bering shelf reported negligible fluxes of DIN, indicating that local regeneration was not an important source of nitrogen to the overlying water (Horak et al., 2013).

Generally, NO_3^- fluxes reported elsewhere in Chukchi Sea were directed both into and out of the sediments (Devol et al. 1997; Henriksen et al., 1993; Horak et al., 2013; Rowe and Phoel, 1992). Devol and colleagues (1997) report both NO_3^- influx and efflux; our absolute uptake rates were higher than theirs, although they reported greater NO_3^- efflux (Table 5). In comparison, Souza and colleagues (2014b) report a small net efflux or uptake of NO_3^- and PO_4^{3-}, with both rates being slower than ours (Table 5). Most of the Greenland and Norway studies surveyed reported NO_3^- efflux, which was cited as evidence of active sediment nitrification (Table 5). Overall, our NO_3^- influx rates are at least three times higher than those in the literature surveyed.

4.1.3 Net sediment denitrification

Net N_2 fluxes measured in this study were always directed out of the sediments, indicating the occurrence of net denitrification, or possibly anammox. Heterotrophic

denitrification is the largest global fixed nitrogen sink (Devol, 2015), with the majority of sedimentary denitrification occurring on continental margins (Christensen et al., 1987; Seitzinger et al., 2006). Anammox is another pathway of NO_2^- reduction that releases N_2 gas and has been detected in continental margins (Thamdrup and Dalsgaard, 2002; Trimmer et al., 2013; Rysgaard et al. 2004). Our companion study using ^{15}N tracers measured anammox at these stations, but denitrification rates exceeded anammox rates by one to two orders of magnitude (McTigue et al., 2016). Our results correspond with the other limited studies of N_2 flux in the Chukchi Sea (Table 5; Fig. 5). For example, Chang and Devol (2009) reported N_2 fluxes of n.d. – 65.8 μmol N m^{-2} d^{-1} at stations ranging from 50 – 1,450 m deep (Table 5; Fig. 5). Their highest rates occurred at the shallowest station, and the authors developed a predictive relationship between N_2 flux and depth. This may reflect the relationship between POC delivery to the seafloor and heterotrophic denitrification since shallower depths are more tightly coupled to water column production.

The current study covers a narrower depth range (41 – 66 m) than Chang and Devol's (2009) study that focused on shelf-basin interactions, but N_2 flux and depth were significantly correlated (Table 4), with highest average rates occurring at the shallowest station (CBL11). Denitrification at our stations may reflect variations in time-integrated POC flux to the sediments, which often correlates with depth (Chang and Devol, 2009). Net N_2 fluxes and DOU correlated negatively with sediment TOC and TN (Table 4, Fig. 4); thus, stations with more organic matter standing stock favored O_2 over NO_3^- respiration. This result may indicate production of H_2S via SO_4^{2-} reduction, which would be favored under high organic carbon loading, and H_2S inhibits nitrification (Joye and Hollibaugh, 1995). Alternatively, these correlations may reflect a relatively fresh deposition of organic carbon at the stations with highest sediment organic content, which would be respired in order of decreasing free energy

yield, first by aerobic heterotrophic bacteria, consuming the most labile fraction of the organic carbon. Over time, the denitrifiers would be left with less labile organic carbon, which would be consumed more slowly. Thus, stations with more recent deposition of sediment organic carbon favored O_2 over NO_3^- respiration, as in other studies (e.g., Chang and Devol, 2009; Sayles et al., 1994).

The largest reported range in N_2 fluxes in the southern and northern Chukchi shelf (Souza et al., 2014b), spanned from net nitrogen fixation to net denitrification, -27 to 286 μmol N m^{-2} h^{-1} (Table 5; Fig. 5). Interestingly, the net nitrogen fixation data was measured closest to Hanna Shoal. However, our data do not support net nitrogen fixation, nor do the other studies measuring N_2 flux in this or other Arctic shelf regions (Table 5; Fig. 5; Chang and Devol, 2009; Devol et al., 1997; Christensen 2008). This topic warrants further investigation.

Denitrifiers can use NO_3^- diffusing into porewater from the overlying water (D_w), or by coupling to nitrification of porewater NH_4^+ to NO_3^- in sediments (D_n). Our observed NO_x fluxes into the sediments suggest that 16 – 65% of denitrification may have occurred via D_w, [NO_x / N_2 x 100%]. This result corresponds well to our estimates of D_w from a ^{15}N tracer study, which ranged from 8 – 42% (McTigue et al., 2016), indicating a dominance of D_n rather than D_w. Previous studies in the Chukchi and Bering Seas also report significant D_n in sediments (Brown et al., 2015; Horak et al., 2013). Coupled D_n can account for up to 80% of total denitrification in continental shelves globally assuming bottom water NO_3^- concentrations < 10 μM, as at our stations (Table 1; Seitzinger et al., 2006). Porewater NH_4^+ concentrations, ranging from 39 – 86 μM, were sufficient to support nitrification and subsequent denitrification (McTigue et al., 2016). For example, porewater NH_4^+ concentrations were relatively replete in the top 5 cm (76.5 ± 10.9 μM) at H33, where we observed the highest NO_x uptake rates and highest D_w proportions.

However, NH_4^+ concentrations near the zone of NO_3^- reduction (OPD = 6.8 mm), may have been more limiting, as concentrations can be depleted near the surface, and overlying NO_3^- concentrations were adequate to support D_w. DIN uptake by microalgae may occur in situ on Hanna Shoal, as light levels are 4-20 μmol photons m^{-2} s^{-1} at the sediment surface (40 – 50 m depth; McTigue and Dunton, 2014), which may be adequate to support photosynthesis of dark-adapted Arctic benthic microalgae (Kuhl et al., 2001). Benthic microalgae capable of dark DIN uptake (Evrard et al., 2008; Rysgaard et al., 1993) may have contributed to our observed DIN influxes. DIN uptake may also represent incorporation into microbial biomass and/or subsequent incorporation into higher trophic levels (Cooper et al., 2015; Denisenko et al., 2015).

4.2 NH_4^+ cycling at the sediment-water interface

No net NH_4^+ flux occurred at H17. The $^{15}NH_4^+$ treatment allowed a more detailed analysis of NH_4^+ cycling at the sediment-water interface. Measurement of net flux alone may underestimate actual NH_4^+ regeneration because NH_4^+ uptake (removal) processes may occur at similar rates as NH_4^+ production, so that the measured net flux is low even though actual regeneration is high (Gardner and McCarthy, 2009). This pattern is demonstrated at station H17, where net flux was zero but both active NH_4^+ regeneration and uptake were of equal magnitude and occurring simultaneously (Fig. 3). In fact, station H17 had the highest rates of actual uptake and one of the highest rates of regeneration. All stations showed active NH_4^+ regeneration, and most showed net release to the overlying water. In many systems, regeneration is a vital internal source of recycled nitrogen that can fuel overlying production, heterotrophic bacteria, and nitrification (Brown et al., 2015; Souza et al., 2014a; Tobias et al., 2003). In agreement with our

third hypothesis, NH_4^+ regeneration correlated negatively with TOU (Table 4), providing evidence that NH_4^+ was produced via heterotrophic remineralization processes.

On Hanna Shoal, net NH_4^+ flux contributed to the DIN pool in the overlying water but was not the primary fate of nitrogen processed in the sediments, as discussed below (Fig. 6). Despite the net release of NH_4^+, all stations except CBL13 showed actual NH_4^+ uptake, indicating use of NH_4^+ by sediment microbes such as nitrifiers. NH_4^+ is also used by some heterotrophic bacteria as an energetically less expensive source of nitrogen than NO_3^- for growth (Grebmeier et al., 2015; Middelburg and Nieuwenhuize, 2000). As predicted by our third hypothesis, actual uptake rates correlated negatively with sediment TOC and TN, such that the highest uptake rates (expressed as a negative value) occurred when sediment organic content was highest. Perhaps NH_4^+ became more limiting as sediment organic content increased. After the addition of $^{15}NH_4^+$, all stations showed additional NH_4^+ uptake, revealing some degree of NH_4^+ limitation at the sediment-water interface, which is quantified as sediment NH_4^+ demand (SAD; Fig. 3d). Although porewater NH_4^+ concentrations were high in the top 5 cm, concentrations may have been more limiting closer to the sediment surface where high rates of uptake by nitrifiers, anammox bacteria, and heterotrophic bacteria removed NH_4^+ more quickly than it could be resupplied via organic matter remineralization. SAD was not correlated with any measured environmental parameters.

Numerous water column and sediment studies have investigated NH_4^+ uptake and regeneration using the $^{15}NH_4^+$ approach (Arrigo and van Dijken, 2015; Brown et al., 2015; Lin et al., 2011; McCarthy et al., 2007; Paerl et al., 2011; Souza et al., 2014a). Previous work in this system demonstrates that close coupling of water column NH_4^+ regeneration and uptake, including the water directly overlying sediments, suggesting rapid NH_4^+ turnover (Souza et al.,

2014a). Nitrification accounted for most of the NH_4^+ uptake in the water column. The measured nitrification rates were comparable to rates measured in the warmer northern Gulf of Mexico (Carini et al., 2010), highlighting the importance of water-column nitrification in this perennially cold Arctic system. Previous work on the Chukchi shelf suggests a decoupling of ammonification and nitrification in the summer as seen by the buildup of NH_4^+ in bottom waters in summer (Brown et al., 2015). The decoupling was due to slower nitrification in summer rather than enhanced ammonification. Although we detected NH_4^+ in bottom waters (<2.6 μM) from sediment remineralization and faunal release, the measured rapid NH_4^+ uptake rates and SAD, along with our estimates of D_n, suggest that nitrification is important in Hanna Shoal sediments. Direct measurements of sediment nitrification in the Chukchi shelf are limited (Henriksen et al., 1993) and more data are needed in this region.

4.3 System-wide nitrogen cycling

Sediments are major sites for nitrogen uptake, transformation, and removal through microbial processes such as aerobic respiration and denitrification. The relative proportion of different forms of nitrogen fluxing into or out of the sediments has important implications for the ecosystem nitrogen budget. Nitrogen released as N_2 gas is lost from the system, whereas nitrogen released as NH_4^+ or NO_x may further stimulate primary production in the overlying water. The Chukchi Sea is one of the gateway seas to the Arctic; water advected northward through the Bering Strait must traverse this platform before entering the rest of the Arctic Ocean. The loss or recycling of inorganic nitrogen here can modulate the productivity of the rest of the Arctic Ocean. N_2 was the largest of the dark nitrogen fluxes, indicating that these sediments are

efficient at removing nitrogen through denitrification (Fig. 6), as predicted in our second hypothesis. Even though most stations released NH_4^+ to the overlying water, they functioned as a net sink for DIN, largely driven by greater NO_x uptake, which may have partially fueled denitrification (Fig. 6).

Denitrification efficiency is a useful term for quantifying the percentage of the total inorganic nitrogen released as N_2 during organic matter decomposition, or $[N_2/(DIN + N_2)]$ x 100% (Berelson et al., 1998; Eyre and Ferguson, 2002). In many systems, the rate of carbon loading influences the efficiency with which the system loses nitrogen as N_2, such that highest denitrification efficiencies correspond to low organic carbon loading and lowest efficiencies (and net NH_4^+ release) occur when labile organic carbon loading is high. Low denitrification efficiencies likely result from sulfide inhibition of nitrification and denitrification (Joye and Hollibaugh, 1995) and/or insufficient O_2 for nitrification. Alternatively, as organic carbon loading increases, DNRA may become relatively more important (Giblin et al., 2013; Hardison et al., 2015). The efficiencies at Hanna Shoal ranged from 69 to 86%, indicating a relatively efficient system for removing nitrogen as N_2 vs. recycling it as bioavailable DIN (Table 2). Denitrification efficiency correlated negatively with TOC and TN, a proxy for organic carbon loading, with highest efficiencies when organic content was lowest (Table 4), indicating similar controls on nitrogen recycling in the Hanna Shoal system as in other regions (Eyre and Ferguson, 2002; Gardner and McCarthy, 2009).

The net release of N_2 gas was the major nitrogen pathway in the sediments, resulting in net removal of nitrogen during the summer (Fig. 6). Denitrification in these perennially cold shelf sediments may not vary seasonally because the timescale on which POC is denitrified is long relative to the seasonal pulses of organic matter; however, there is a paucity of

denitrification data from the Chukchi Sea, so these Hanna Shoal rates can inform our limited knowledge of denitrification in this region. A previous study of denitrification in this system suggests that denitrification rates vary little from ice-covered spring to ice-free summer (Chang and Devol, 2009) and between summer and winter (Devol et al. 1997); thus, we would expect our results to extend to spring and winter. Our N_2 production rates were similar to those measured in the Chukchi region and slightly higher than those measured in other areas of the Arctic (Table 5; Fig. 5), and we would expect similar results in as yet unstudied Arctic shelf regions with similar depth and primary productivity. Although our stations cover too little space to scale up our findings to a broader context, our results combined with those surveyed in the literature suggest that, despite the cold temperatures, Arctic continental shelves are important nitrogen loss regions to consider for constructing global nitrogen budgets.

4.4 System-wide organic carbon remineralization

Sediment O_2 uptake is useful for assessing benthic organic carbon mineralization during early diagenesis (Arrigo and van Dijken, 2011; Glud et al., 1994; Glud, 2008; Wenzhofer and Glud, 2002). We can estimate the amount of organic carbon mineralized in these sediments by benthic bacteria and fauna if we consider TOU. O_2 consumption rates were converted to carbon respiration rate units using a respiratory quotient of 122 moles of C respired to 175 moles of O_2 consumed (Moran et all, 2005; Grebmeier et al., 2006). This ratio assumes that most sediment respiration is due to macrobenthic infauna, and that rates of microbial anoxic respiration are relatively low (Grebmeier et al., 2006). Benthic carbon remineralization rates ranged from 109 ± 8 to 315 ± 116 μmol C m^{-2} h^{-1} (Table 6). These values account for approximately 34 ± 9% (range

20 - 57%) of summer export production (13.2 ± 13.0 mmol C m^{-2} d^{-1}) measured previously on the northern Chukchi shelf (Table 6; Moran et al., 2005). POC export accounted for ~37 % of summer primary production on the shelf (Moran et al., 2005). Previous estimates of POC export and benthic carbon remineralization on the shelf showed a strong correspondence at shallow (<300 m) stations, indicating strong benthic-pelagic coupling, relative to deeper slope stations (Moran et al., 2005). Benthic carbon respiration accounted for ~55% of export production in the summer, which is greater than our estimate; their study postulated that much of the carbon not being remineralized in the sediments was exported at the shelf-break region (Moran et al., 2005).

The amount of organic carbon oxidized via denitrification can be estimated using the reaction stoichiometry of the complete denitrification pathway, from NO_3^- reduction to N_2 gas production: $NO_3^- + 1.25CH_2O \rightarrow 0.5N_2 + 1.25HCO_3^- + 0.25H^+$ (see Hardison et al., 2015). Assuming stoichiometry of 1N:1.25C yields carbon mineralization rates of 30 ± 5 to 69 ± 3 μmol C m^{-2} h^{-1} (Table 6). These values account for approximately 6 - 12% of summer export production measured on the northern Chukchi shelf (Moran et al., 2005). Denitrification accounted for 17 – 36% of the total carbon oxidation (Fig. 6). These percentages reflect global trends, as O_2 is responsible for more than 80% of total organic carbon oxidation in continental shelf sediments (Lefevre et al., 1997; Martin and Sayles, 2003). Denitrification at Hanna Shoal and elsewhere in the productive Chukchi Sea may be enhanced relative to global averages due to the high abundance of benthic infauna (Dunton et al., 2005; Grebmeier et al., 2015; Schonberg et al., 2014), which enhance denitrification via bioirrigation and bioturbation activities that expand the zone of NO_3^- reduction (Braeckman et al., 2014; Kristensen et al., 1991; McTigue et al., 2016). Thus, these shallow, productive Arctic shelves may be local “hotspots” for organic carbon remineralization.

5. Conclusions

Sediments of the highly productive Hanna Shoal region of the Chukchi Sea are sites of active O_2 respiration and denitrification. Approximately 34% of summer export production is remineralized via benthic faunal and microbial respiration, with ~25% of the carbon oxidized via denitrification. Despite net release of NH_4^+ to the overlying water, the sediments act as a net nitrogen sink via denitrification, which is fueled both by NO_3^- from the overlying water (D_w) and by nitrification of porewater NH_4^+ (D_n). The Arctic region is expected to change dramatically as a result of climate change, including reduction of summer sea ice, and seawater warming and freshening (Arrigo, 2015; Grebmeier et al., 2015). The consequences of climate change on biogeochemical cycling in this and other Arctic shelf regions are unknown. Some have hypothesized that warming and longer ice-free periods will increase organic carbon production and export (Arrigo, 2015; Sørensen et al., 2015), which may fuel sediment organic carbon remineralization, including denitrification and associated nitrogen removal, while others predict that increased stratification could lead to nutrient depletion and a reduction in overall production (Grebmeier et al., 2006). These shallow productive Arctic shelves are "hotspots" for organic carbon remineralization and associated nitrogen cycling processes that warrant consideration in global analyses of these processes under current and future climate conditions.

6. Acknowledgments

We are grateful to the captain and crew of the USCGC *Healy* for the productive and safe research voyage, HLY1301. We thank M. McCarthy for helpful discussion of $^{15}NH_4^+$ data, K. Liu for analyzing AIRTS samples, N. Reyna and A. Wohlrab for assistance with nutrient analyses, P. Bucolo for assistance with the O_2 microprofiles, C. Algar for assistance with O_2 microprofile code, H. Wei for creating Fig. 1, and Z. Liu for running pigment samples. We are also thankful to two anonymous reviewers for their helpful comments on this manuscript. This study was funded by the U.S. Department of the Interior, Bureau of Ocean Energy Management (BOEM), Alaska Outer Continental Shelf Region, Anchorage, Alaska under BOEM Cooperative Agreement No. M11AC00007 as part of the Chukchi Sea Offshore Monitoring in Drilling Area (COMIDA) and through support by the National Science Foundation under Grant No. EAR-1417433 to AKH.

7. References

Archer, D., Devol, A., 1992. Benthic Oxygen Fluxes on the Washington Shelf and Slope - a Comparison of In situ Microelectrode and Chamber Flux Measurements. Limnology and Oceanography 37, 614-629.

Arrigo, K.R., 2015. Impacts of Climate on EcoSystems and Chemistry of the Arctic Pacific Environment (ICESCAPE). Deep-Sea Research Part Ii-Topical Studies in Oceanography 118, 1-6.

Arrigo, K.R., van Dijken, G.L., 2011. Secular trends in Arctic Ocean net primary production. Journal of Geophysical Research-Oceans 116.

Arrigo, K.R., van Dijken, G.L., 2015. Continued increases in Arctic Ocean primary production. Progress in Oceanography 136, 60-70.

Bauer, J.E., Cai, W.J., Raymond, P.A., Bianchi, T.S., Hopkinson, C.S., Regnier, P.A.G., 2013. The changing carbon cycle of the coastal ocean. Nature 504, 61-70.

Berelson, W.M., Heggie, D., Longmore, A., Kilgore, T., Nicholson, G., Skyring, G., 1998. Benthic nutrient recycling in Port Phillip Bay, Australia. Estuarine Coastal and Shelf Science 46, 917-934.

Blackburn, T.H., 1979. Method for Measuring Rates of NH_4^+ Turnover in Anoxic Marine-Sediments, Using a N-15- NH_4^+ Dilution Technique. Applied and Environmental Microbiology 37, 760-765.

Boudreau, B.P., 1997. Diagenetic Models and Their Implementation: Modelling Transport and Reactions in Aquatic Sediments. Springer.

Braeckman, U., Foshtomi, M.Y., Van Gansbeke, D., Meysman, F., Soetaert, K., Vincx, M., Vanaverbeke, J., 2014. Variable Importance of Macrofaunal Functional Biodiversity for Biogeochemical Cycling in Temperate Coastal Sediments. Ecosystems 17, 720-737.

Brown, Z.W., Casciotti, K.L., Pickart, R.S., Swift, J.H., Arrigo, K.R., 2015. Aspects of the marine nitrogen cycle of the Chukchi Sea shelf and Canada Basin. Deep-Sea Research Part II-Topical Studies in Oceanography 118, 73-87.

Brin, L.D., Giblin, A.E. Rich, J.J., 2014. Environmental controls of anammox and denitrification in southern New England estuarine and shelf sediments. Limnology and Oceanography 59, 851-860.

Canfield, D.E., Jørgensen, B.B., Fossing, H., Glud, R., Gundersen, J., Ramsing, N.B., Thamdrup, B., Hansen, J.W., Nielsen, L.P. Hall, P.O., 1993. Pathways of organic carbon oxidation in three continental margin sediments. Marine Geology 113, 27-40.

Carini, S.A., McCarthy, M.J., Gardner, W.S., 2010. An isotope dilution method to measure nitrification rates in the northern Gulf of Mexico and other eutrophic waters. Continental Shelf Research 30, 1795-1801.

Chang, B.X., Devol, A.H., 2009. Seasonal and spatial patterns of sedimentary denitrification rates in the Chukchi sea. Deep-Sea Research Part II-Topical Studies in Oceanography 56, 1339-1350.

Christensen, J.P., 2008. Sedimentary carbon oxidation and denitrification on the shelf break of the Alaskan Beaufort and Chukchi Seas. The Open Oceanography Journal 2, 6-17.

Christensen, B., Vedel, A., Kristensen, E., 2000. Carbon and nitrogen fluxes in sediment inhabited by suspension-feeding (Nereis diversicolor) and non-suspension-feeding (N-virens) polychaetes. Marine Ecology Progress Series 192, 203-217.

Christensen, J.P., Murray, J.W., Devol, A.H., Codispoti, L.A., 1987. Denitrification in continental shelf sediments has major impact on the ocean nitrogen budget. Global Biiogeochemical Cycles 1, 97-116.

Codispoti, L.A., Kelly, V., Thessen, A., Matrai, P., Suttles, S., Hill, V., Steele, M., Light, B., 2013. Synthesis of primary production in the Arctic Ocean: III. Nitrate and phosphate based estimates of net community production. Progress in Oceanography 110, 126-150.

Cooper, L.W., Savvichev, A.S., Grebmeier, J.M., 2015. Abundance and Production Rates of Heterotrophic Bacterioplankton in the Context of Sediment and Water Column Processes in the Chukchi Sea. Oceanography 28, 84-99.

Denisenko, S.G., Grebmeier, J.M., Cooper, L.W., 2015. Assessing Bioresources and Standing Stock of Zoobenthos (Key Species, High Taxa, Trophic Groups) in the Chukchi Sea. Oceanography 28, 146-157.

Devol, A.H., 2015. Denitrification, Anammox, and N_2 Production in Marine Sediments. Annual Review of Marine Science, Vol 7 7, 403-423.

Devol, A.H., Codispoti, L.A., Christensen, J.P., 1997. Summer and winter denitrification rates in western Arctic shelf sediments. Continental Shelf Research 17, 1029-.

Dunton, K.H., Goodall, J.L., Schonberg, S.V., Grebmeier, J.M., Maidment, D.R., 2005. Multi-decadal synthesis of benthic-pelagic coupling in the western arctic: Role of cross-shelf advective processes. Deep-Sea Research Part II-Topical Studies in Oceanography 52, 3462-3477.

Dunton, K.H., Saupe, S.M., Golikov, A.N., Schell, D.M., Schonberg, S.V., 1989. Trophic Relationships and Isotopic Gradients among Arctic and Subarctic Marine Fauna. Marine Ecology Progress Series 56, 89-97.

Evrard, V., Cook, P.L.M., Veuger, B., Huettel, M., Middelburg, J.J., 2008. Tracing carbon and nitrogen incorporation and pathways in the microbial community of a photic subtidal sand. Aquatic Microbial Ecology 53, 257-269.

Eyre, B.D., Ferguson, A.J.P., 2002. Comparison of carbon production and decomposition, benthic nutrient fluxes and denitrification in seagrass, phytoplankton, benthic microalgae- and macroalgae-dominated warm-temperate Australian lagoons. Marine Ecology Progress Series 229, 43-59.

Gardner, C.W., 1995. High-Performance Liquid-Chromatography - an Introduction to the Chemistry of HPLC. Abstracts of Papers of the American Chemical Society 209, 23-TECH.

Gardner, W.S., McCarthy, M.J., 2009. Nitrogen dynamics at the sediment-water interface in shallow, sub-tropical Florida Bay: why denitrification efficiency may decrease with increased eutrophication. Biogeochemistry 95, 185-198.

Gardner, W.S., McCarthy, M.J., Carini, S.A., Souza, A.C., Lijun, H., McNeal, K.S., Puckett, M.K., Pennington, J., 2009. Collection of intact sediment cores with overlying water to study nitrogen- and oxygen-dynamics in regions with seasonal hypoxia. Continental Shelf Research 29, 2207-2213.

Giblin, A.E., Tobias, C.R., Song, B., Weston, N., Banta, G.T., Rivera-Monroy, V.H., 2013. The Importance of Dissimilatory Nitrate Reduction to Ammonium (DNRA) in the Nitrogen Cycle of Coastal Ecosystems. Oceanography 26, 124-131.

Glud, R.N., 2008. Oxygen dynamics of marine sediments. Marine Biology Research 4, 243-289.

Glud, R.N., Risgaard-Petersen, N., Thamdrup, B., Fossing, H., Rysgaard, S., 2000. Benthic carbon mineralization in a high-Arctic sound (Young Sound, NE Greenland). Marine Ecology Progress Series 206, 59-71.

Glud, R.N., Holby, O., Hoffmann, F. Canfield, D.E., 1998. Benthic mineralization and exchange in Arctic sediments (Svalbard, Norway). Marine Ecology Progress Series 173, 237-251.

Glud, R.N., Gundersen, J.K., Jorgensen, B.B., Revsbech, N.P., Schulz, H.D., 1994. Diffusive and Total Oxygen-Uptake of Deep-Sea Sediments in the Eastern South-Atlantic Ocean - in-Situ and Laboratory Measurements. Deep-Sea Research Part I-Oceanographic Research Papers 41, 1767-1788.

Grebmeier, J.M., Bluhm, B.A., Cooper, L.W., Danielson, S.L., Arrigo, K.R., Blanchard, A.L., Clarke, J.T., Day, R.H., Frey, K.E., Gradinger, R.R., Kedra, M., Konar, B., Kuletz, K.J., Lee, S.H., Lovvorn, J.R., Norcross, B.L., Okkonen, S.R., 2015. Ecosystem characteristics and processes facilitating persistent macrobenthic biomass hotspots and associated benthivory in the Pacific Arctic. Progress in Oceanography 136, 92-114.

Grebmeier, J.M., Cooper, L.W., Feder, H.M., Sirenko, B.I., 2006. Ecosystem dynamics of the Pacific-influenced Northern Bering and Chukchi Seas in the Amerasian Arctic. Progress in Oceanography 71, 331-361.

Gruber, N., Sarmiento, J.L., 1997. Global patterns of marine nitrogen fixation and denitrification. Global Biogeochemical Cycles 11, 235-266.

Hardison, A.K., Algar, C.K., Giblin, A.E., Rich, J.J., 2015. Influence of organic carbon and nitrate loading on partitioning between dissimilatory nitrate reduction to ammonium (DNRA) and N_2 production. Geochimica et Cosmochimica Acta 164, 146-160.

Henriksen, K., Blackburn, T.H., Lomstein, B.A., Mcroy, C.P., 1993. Rates of Nitrification, Distribution of Nitrifying Bacteria and Inorganic N Fluxes in Northern Bering Chukchi Shelf Sediments. Continental Shelf Research 13, 629-651.

Horak, R.E.A., Whitney, H., Shull, D.H., Mordy, C.W., Devol, A.H., 2013. The role of sediments on the Bering Sea shelf N cycle: Insights from measurements of benthic denitrification and benthic DIN fluxes. Deep-Sea Research Part II-Topical Studies in Oceanography 94, 95-105.

Joye, S.B., Anderson, I.C., 2008. Nitrogen cycling in coastal sediments, in: Capone, D.G., Bronk, D.A., Mulholland, M.R., Carpenter, E.J. (Eds.), Nitrogen in the Marine Environment, 2 ed. Academic Press, pp. 867-915.

Joye, S.B., Hollibaugh, J.T., 1995. Influence of Sulfide Inhibition of Nitrification on Nitrogen Regeneration in Sediments. Science 270, 623-625.

Kana, T.M., Darkangelo, C., Hunt, M.D., Oldham, J.B., Bennett, G.E., Cornwell, J.C., 1994. Membrane Inlet Mass-Spectrometer for Rapid High-Precision Determination of N_2, O_2, and Ar in Environmental Water Samples. Analytical Chemistry 66, 4166-4170.

Kristensen, E., Jensen, M.H., Aller, R.C., 1991. Direct Measurement of Dissolved Inorganic Nitrogen Exchange and Denitrification in Individual Polychaete (Nereis-Virens) Burrows. Journal of Marine Research 49, 355-377.

Kuhl, M., Glud, R.N., Borum, J., Roberts, R., Rysgaard, S., 2001. Photosynthetic performance of surface-associated algae below sea ice as measured with a pulse-amplitude-modulated (PAM) fluorometer and O_2 microsensors. Marine Ecology Progress Series 223, 1-14.

Lavrentyev, P.J., Gardner, W.S., Yang, L.Y., 2000. Effects of the zebra mussel on nitrogen dynamics and the microbial community at the sediment-water interface. Aquatic Microbial Ecology 21, 187-194.

Lefevre, D., Minas, H.J., Minas, M., Robinson, C., Williams, P.J.L., Woodward, E.M.S., 1997. Review of gross community production, primary production, net community production and dark community respiration in the Gulf of Lions. Deep-Sea Research Part II-Topical Studies in Oceanography 44, 801-.

Lin, X.A., McCarthy, M.J., Carini, S.A., Gardner, W.S., 2011. Net, actual, and potential sediment-water interface NH_4^+ fluxes in the northern Gulf of Mexico (NGOMEX): Evidence for NH_4^+ limitation of microbial dynamics. Continental Shelf Research 31, 120-128.

Martin, W.R., Sayles, F.L., 2003. The Recycling of Biogenic Material at the Seafloor, in: Mackenzie, F.T., Holland, H.D., Turekian, K.K. (Eds.), Treatise on Geochemistry. Elsevier, pp. 37-65.

McCarthy, M.J., Gardner, W.S., Lavrentyev, P.J., Moats, K.M., Joehem, F.J., Klarer, D.M., 2007. Effects of hydrological flow regime on sediment-water interface and water column nitrogen dynamics in a great lakes coastal wetland (Old Woman Creek, Lake Erie). J Great Lakes Res 33, 219-231.

McTigue, N.D., Bucolo, P., Liu, Z.F., Dunton, K.H., 2015. Pelagic-benthic coupling, food webs, and organic matter degradation in the Chukchi Sea: Insights from sedimentary pigments and stable carbon isotopes. Limnology and Oceanography 60, 429-445.

McTigue, N.D., Dunton, K.H., 2014. Trophodynamics and organic matter assimilation pathways in the northeast Chukchi Sea, Alaska. Deep-Sea Research Part II-Topical Studies in Oceanography 102, 84-96.

McTigue, N.D., Gardner, W.S., Dunton, K.H., Hardison, A.K., 2016. Biotic and abiotic controls on co-occurring denitrification, anammox, and DNRA in shallow Arctic shelf sediments. Nat Commun.

Michaud, E., Desrosiers, G., Mermillod-Blondin, F., Sundby, B., Stora, G., 2005. The functional group approach to bioturbation: The effects of biodiffusers and gallery-diffusers of the Macoma balthica community on sediment oxygen uptake. Journal of Experimental Marine Biology and Ecology 326, 77-88.

Middelburg, J.J., Nieuwenhuize, J., 2000. Nitrogen uptake by heterotrophic bacteria and phytoplankton in the nitrate-rich Thames estuary. Marine Ecology-Progress Series 203, 13-21.

Mooney, R.F., McClelland, J.W., 2012. Watershed Export Events and Ecosystem Responses in the Mission-Aransas National Estuarine Research Reserve, South Texas. Estuaries and Coasts 35, 1468-1485.

Moran, S.B., Kelly, R.P., Hagstrom, K., Smith, J.N., Grebmeier, J.M., Cooper, L.W., Cota, G.F., Walsh, J.J., Bates, N.R., Hansell, D.A., Maslowski, W., Nelson, R.P., Mulsow, S., 2005. Seasonal changes in POC export flux in the Chukchi Sea and implications for water column-

benthic coupling in Arctic shelves. Deep-Sea Research Part Ii-Topical Studies in Oceanography 52, 3427-3451.

Nixon, S., 1981. Remineralization and nutrient cycling in coastal marine ecosystems, in: Neilson, B., Cronin, L. (Eds.), Estuaries and Nutrients. Humana Press, Clifton, NJ, pp. 111-138.

Paerl, H.W., Xu, H., McCarthy, M.J., Zhu, G.W., Qin, B.Q., Li, Y.P., Gardner, W.S., 2011. Controlling harmful cyanobacterial blooms in a hyper-eutrophic lake (Lake Taihu, China): The need for a dual nutrient (N & P) management strategy. Water Research 45, 1973-1983.

Reimers, C., Jahnke, R.A., Thomson, L., 2001. In situ sampling in the benthic boundary layer, in: Boudreau, B.P., Jorgensen, B.B. (Eds.), The Benthic Boundary Layer--Transport Processes and Biogeochemistry. Oxford University Press, Oxford, pp. 245-268.

Risgaard-Petersen, N., 2004. Denitrification, in: Nielsen, S., Banta, G., Pedersen, M. (Eds.), Estuarine Nutrient Cycling: The Influence of Primary Producers. Kluwer Academic Publishers, The Netherlands, pp. 263-280.

Rowe, G.T., Phoel, W.C., 1992. Nutrient Regeneration and Oxygen-Demand in Bering Sea Continental-Shelf Sediments. Continental Shelf Research 12, 439-449.

Rysgaard, S., Risgaard-Petersen, N., Nielsen, L.P., Revsbech, N.P., 1993. Nitrification and Denitrification in Lake and Estuarine Sediments Measured by the N-15 Dilution Technique and Isotope Pairing. Applied and Environmental Microbiology 59, 2093-2098.

Rysgaard, S., Glud, R.N., Risgaard-Petersen, N. Dalsgaard, T., 2004. Denitrification and anammox activity in Arctic marine sediments. Limnology and Oceanography 49, 1493-1502.

Sayles, F.L., Martin, W.R., Deuser, W.G., 1994. Response of Benthic Oxygen-Demand to Particulate Organic-Carbon Supply in the Deep-Sea near Bermuda. Nature 371, 686-689.

Schonberg, S.V., Clarke, J.T., Dunton, K.H., 2014. Distribution, abundance, biomass and diversity of benthic infauna in the Northeast Chukchi Sea, Alaska: Relation to environmental variables and marine mammals. Deep-Sea Research Part II-Topical Studies in Oceanography 102, 144-163.

Seitzinger, S., Harrison, J.A., Bohlke, J.K., Bouwman, A.F., Lowrance, R., Peterson, B., Tobias, C., Van Drecht, G., 2006. Denitrification across landscapes and waterscapes: A synthesis. Ecological Applications 16, 2064-2090.

Smith, S.V., Hollibaugh, J.T., 1993. Coastal Metabolism and the Oceanic Organic-Carbon Balance. Rev Geophys 31, 75-89.

Soetaert, K., Meysman, F., 2009. ReacTran: Reactive transport modeling in 1D, 2D, and 3D, R package version 2.1. Available from http://cran.r-project.org/web/packages/ReacTran/index.html. ed.

Soetaert, K., Petzoldt, T., 2012. FME: A flexible modelling environment for inverse modelling, sensitivity, identifiability, Monte Carlo analysis. R package version 2.6. Available from http://cran.r-project.org/web/packages/FME/index.html

Sørensen, H.L., Meire, L., Juul-Pedersen, T., De Stigter, H.C., Meysman, F.J., Rysgaard, S., Thamdrup, B. Glud, R.N., 2015. Seasonal carbon cycling in a Greenlandic fjord: an integrated pelagic and benthic study. Marine Ecology Progress Series 539, 1-17.

Souza, A.C., Gardner, W.S., Dunton, K.H., 2014a. Rates of nitrification and ammonium dynamics in northeastern Chukchi Sea shelf waters. Deep-Sea Research Part II-Topical Studies in Oceanography 102, 68-76.

Souza, A.C., Kim, I.N., Gardner, W.S., Dunton, K.H., 2014b. Dinitrogen, oxygen, and nutrient fluxes at the sediment-water interface and bottom water physical mixing on the eastern Chukchi Sea shelf. Deep-Sea Research Part II-Topical Studies in Oceanography 102, 77-83.

Thamdrup, B., Dalsgaard, T., 2002. Production of N_2 through anaerobic ammonium oxidation coupled to nitrate reduction in marine sediments. Applied and Environmental Microbiology 68, 1312-1318.

Tobias, C., Giblin, A., McClelland, J., Tucker, J., Peterson, B., 2003. Sediment DIN fluxes and preferential recycling of benthic microalgal nitrogen in a shallow macrotidal estuary. Marine Ecology-Progress Series 257, 25-36.

Trimmer, M., Engstrom, P., Thamdrup, B., 2013. Stark Contrast in Denitrification and Anammox across the Deep Norwegian Trench in the Skagerrak. Applied and Environmental Microbiology 79, 7381-7389.

Wenzhofer, F., Glud, R.N., 2002. Benthic carbon mineralization in the Atlantic: a synthesis based on in situ data from the last decade. Deep-Sea Research Part I-Oceanographic Research Papers 49, 1255-1279.

Figure Captions

Figure 1. Study area. Sample stations across Hanna Shoal in the Northeast Chukchi Sea, Alaska. Depth contour lines are 10 m increments. Dark grey color in lower right quadrant denotes Alaska mainland, with major cities indicated.

Figure 2. Gas and nutrient fluxes. Gas (O_2, N_2) and nutrient (NH_4^+, PO_4^{3-}, NO_3^-, NO_2^-) fluxes at the sediment-water interface measured in control cores. O_2 units are μmol O_2 m^{-2} h^{-1}, nitrogen units are μmol N m^{-2} h^{-1}, and PO_4^{3-} units are μmol P m^{-2} h^{-1}. Vales are mean (SE) for duplicate cores. In panel A, grey bars correspond to total O_2 utilization (TOU) from core incubations while circles correspond to diffusive O_2 utilization (DOU) from microelectrode profiles from cores. Letters in italics designate groups from a post-hoc Tukey's test. Means with the same letter are not significantly different. In panel A, letters correspond to TOU values. DOU values were not statistically different from one another.

Figure 3. NH_4^+ cycling rates. NH_4^+ cycling rates (μmol N m^{-2} h^{-1}) at the sediment-water interface measured in $^{15}NH_4^+$ treated cores. Vales are mean (SE) for duplicate cores. Letters in italics designate groups from a post-hoc Tukey's test. Means with the same letter are not significantly different. REG = regeneration; U_{pot} = potential uptake; U_{act} = actual uptake; SAD = sediment NH_4^+ demand.

Figure 4. Gas fluxes vs. TOC. Relationship between measured TOU, DOU, N_2 fluxes (umol m^{-2} h^{-1}) and sediment TOC content (%). Rates are mean (SE) for duplicate cores. The line in each panel is the linear regression through the points. Correlation values for the relationships are in Table 5.

Figure 5. Comparison with literature values. Comparison of (A) TOU and (B) N_2 fluxes measured in our and other studies in the Arctic. Studies above the dashed grey line are from the Chukchi Sea region, and studies below the line are from the Greenland and Norwegian Arctic. Note that European studies in panel B used the isotope pairing technique (IPT) rather than net N_2 fluxes, as in our study, so the rates should be compared with some caution. Citations: (1) Christensen, 2008; (2) Souza et al., 2014b; (3) Brown et al., 2015; (4) Devol et al., 1997; (5) Grebmeier et al., 2006; (6) Glud et al., 1998; (7) Rysgaard et al., 2004; (8) Glud et al., 2000; (9) Sorensen et al., 2015; (10) Chang and Devol, 2009.

Figure 6. Conceptual diagram. Conceptual diagram of summer nitrogen cycling and organic carbon remineralization in Hanna Shoal sediments. Nitrogen cycling rate units are μmol N m^{-2} h^{-1}, and organic carbon mineralization rate units are μmol C m^{-2} h^{-1}. Values are station mean (SE). NO_x = NO_2^- + NO_3^-; DIN = dissolved inorganic nitrogen; D_n = coupled nitrification-denitrification; D_w = direct denitrification.

Table 1.

Characterization of bottom water and surface sediment. DO = dissolved O_2; TOC = total organic carbon; TN = total nitrogen; Chl *a* = chlorophyll *a*. Sediment TOC, TN, and benthic chlorophyll *a* were measured in top 2 cm. O_2 penetration depth are mean (SE) of duplicate cores. Bottom row is mean (SE) of stations. Additional site metadata can be found in McTigue et al., 2016.

Station	Depth	Bottom temp.	Bottom salinity	Bottom DO	Bottom NH_4^+	Bottom NO_3^-	Sediment TOC	Sediment TN	Benthic Chl *a*	O_2 penetration depth
	m	*°C*		*%*	*µM*	*µM*	*%*	*%*	*mg m^{-2}*	*mm*
CBL11	47	-1.6	32.7	84	2.6	5.2	0.9	0.14	15.0	6.1 (0.8)
CBL13	50	-1.7	32.7	74	1.6	4.7	1.8	0.23	35.2	5.5 (0.5)
H17	41	-1.6	32.7	83	1.7	5.1	0.7	0.09	10.2	5.8 (1.9)
H29	66	-1.6	32.8	79	1.4	5.5	1.5	0.21	8.3	7.6 (0.2)
H33	50	-1.7	32.7	76	2.4	6.8	1.2	0.15	15.4	6.8 (0.7)
Station mean (SE)		-1.6 (0.02)	32.7 (0.02)	79 (2)	1.9 (0.2)	5.5 (0.4)	1.2 (0.2)	0.2 (0.03)	16.8 (4.8)	6.4 (1.2)

Table 2.

Gas and nutrient benthic fluxes in control cores. Values are mean (SE) for duplicate cores. Gas data from MIMS is unavailable for station H17 due to instrument malfunction. DOU = diffusive O_2 uptake; TOU = total O_2 uptake; DIN = dissolved inorganic nitrogen; DNF eff. = denitrification efficiency. Bottom row is mean (SE) of stations.

Station	DOU	TOU	TOU: DOU	N_2	NH_4^+	NO_3^-	NO_2^-	DIN	PO_4^{3-}	DNF eff.
	μmol O_2 m^{-2} h^{-1}			*μmol m^{-2} h^{-1}*						*%*
CBL11	-139 (43)	-277 (32)	2.0 (0.7)	55 (3)	6.3 (2.3)	-8.2 (4.4)	0.5 (0.3)	1.5 (4.0)	2.2 (1.4)	86 (3)
CBL13	-222 (33)	-157 (11)	0.7 (0.1)	28 (4)	10.7 (3.6)	-9.0 (2.0)	-0.3 (0.2)	1.3 (3.4)	0.8 (0.3)	69 (4)
H17	-177 (76)	-	-	-	-0.1 (4.3)	-6.1 (5.9)	-0.7 (0.09)	-6.1 (4.4)	-0.5 (0.5)	-
H29	-201 (4)	-176 (33)	0.9 (0.2)	24 (4)	2.3 (1.7)	-3.8 (0.9)	0.03 (0.09)	-0.5 (2.2)	3.3 (1.2)	86 (4)
H33	-158 (25)	-452 (166)	2.9 (1.2)	43 (8)	3.5 (3.1)	-23 (7.5)	-0.3 (0.3)	-14.8 (8.8)	1.6 (0.8)	82 (6)
Station mean (SE)	-179 (15)	-266 (68)	1.6 (0.4)	38 (7)	4.5 (1.9)	-10 (3.4)	-0.2 (0.2)	-3.7 (3.1)	1.5 (0.6)	81 (5)

Table 3.

NH_4^+ recycling rates from $^{15}NH_4^+$ cores. NET rates are from control cores. Values are mean (SE) for duplicate cores. Units are μmol N m^{-2} h^{-1}. NET = net NH_4^+ flux; REG = regeneration; U_{pot} = potential uptake; U_{act} = actual uptake; SAD = sediment NH_4^+ demand. Bottom row is mean (SE) of stations.

Station	NET	REG	U_{pot}	U_{act}	SAD
CBL11	6.3 (2.3)	14.9 (4.0)	-47.6 (20.2)	-11.3 (4.1)	36.3 (21.6)
CBL13	10.7 (3.6)	6.6 (1.3)	-39.7 (19.0)	6.2 (4.5)	45.9 (20.5)
H17	-0.1 (4.3)	13.5 (4.9)	-36.8 (24.1)	-17.1 (8.6)	19.7 (22.6)
H29	2.3 (1.7)	5.3 (1.8)	-38.7 (18.1)	-1.6 (1.6)	37.0 (18.0)
H33	3.5 (3.1)	12.3 (5.1)	-15.5 (13.2)	-4.9 (4.1)	9.1 (16.8)
Station mean (SE)	4.5 (1.9)	10.5 (1.9)	-35.7 (5.4)	-5.7 (4.0)	29.6 (6.6)

Table 4.

Pearson Correlation coefficients (R) between benthic fluxes and environmental parameters. Values in bold are significance at the p<0.05 level. An asterisk (*) indicates significance at the p<0.01 level. DO = dissolved O_2; TOC = total organic carbon; TN = total nitrogen; TOU = total O_2 uptake; DOU = diffusive O_2 uptake; chl *a* = chlorophyll *a*; DNF eff. = denitrification efficiency; REG = regeneration; U_{pot} = potential uptake; U_{act} = actual uptake; SAD = sediment NH_4^+ demand.

	Depth	Bottom water DO	Sediment TOC	Sediment TN	Benthic chl *a*	TOU	DOU
N_2	**-0.47***	0.34	**-0.6***	**-0.61***	-0.12	**-0.7***	**0.93**
TOU	0.25	-0.09	**0.38**	**0.49***	0.2	1	-0.72
DOU	-0.4	0.58	-0.73	-0.7	-0.51	-0.72	1
NO_2^-	0.19	0.16	0.05	0.14	-0.05	-0.47	0.41
NO_3^-	0.1	0.26	-0.03	0.05	-0.06	0.09	-0.38
NH_4^+	0	-0.21	0.27	0.28	**0.38**	-0.24	-0.32
PO_4^{3-}	**0.43***	-0.04	0.21	0.27	-0.13	-0.03	0.09
REG	-0.32	0.25	-0.36	-0.36	-0.13	**-0.46**	**0.88**
U_{pot}	0	0.16	0.03	-0.3	-0.02	-0.22	0.12
U_{act}	0.34	**-0.52***	**0.61***	**0.59***	**0.43**	0	-0.70
SAD	0.1	0	0.15	0.2	0.15	0.19	-0.54
DNF eff.	0.24	**0.56***	**-0.52**	**-0.45**	**-0.66***	-0.17	0.68

Table 5.

Literature comparison of N_2, O_2, and nutrient fluxes in this and other studies in the Arctic. Studies above dashed line are from the Chukchi Sea region, and studies below the line are from the Greenland and Norwegian Arctic. *Note that European studies used the isotope pairing technique (IPT) rather than the net N_2 fluxes, as in the current study, so the rates should be compared with some caution.

Location	Depth	Season/year	N_2	TOU	NO_3^-	NH_4^+	PO_4^{3-}	Citation
	m				*μmol m^{-2} h^{-1}*			
Hanna Shoal	**41 - 66**	**summer 2013**	**24 – 55**	**-157 – -452**	**-3.8 – -23**	**-0.1 – 10.7**	**-0.5 – 3.3**	***this study***
Chukchi shelf	50 - 1450	spring 2004	n.d. – 65.8	-	-	-	-	Chang & Devol 2009
Chukchi shelf	34 - 46	summer 2010	-27 – 286	-150 – -569	-0.8 – 4.1	-	-1.1 – 13.2	Souza et al. 2014b
Chukchi shelf	11 - 48	summer 1992, winter 1993	0.03 – 0.2	-688 – -825	-6.3 – 27	-1.7 – 31.3	-	Devol et al. 1997
Chukchi & Beaufort shelf-slope	50 - 3894	summer 2004	12.2 – 105.6	-9 – -355	-	-	-	Christensen 2008
N. Chukchi shelf	50 - 200	spring, summer	-	-125 – -1667	-	-	-	Grebmeier et al. 2006
Chukchi shelf	<200	summer 2010, 2011	-	513	-	-	-	Brown et al. 2015
Norway fjords (Svalbard)	115 – 329	fall 1995	6.7 – 26.3*	-150 – -338	5.8 – 11.7	0 – 0.8	-	Glud et al. 1998
Greenland fjord (Young Sound)	20 – 163	summer 1996	4.6 – 20*	-150 – -845	-8.3 – 4.2	1.3 – 18.3	0.4 – 7.5	Glud et al. 2000
Greenland shelf	36 – 100	spring, summer, fall 2001-2003	1.4 – 14*	-141 – -346	0.3 – 10	-	-	Rysgaard et al. 2004
Greenland fjord	110	monthly 2011-2012	8.3 – 25*	-229 – -475	-	-	-	Sorensen et al. 2015

Table 6.

Organic carbon remineralization estimates. Carbon mineralization estimate from TOU uses 175O:122C (Grebmeier et al., 2006). Carbon oxidation via denitrification uses ratio of 1N:1.25C (Hardison et al., 2015). Percent of export production is based on summer export production in Chukchi Sea = 13.2 +/- 13 mmol C m^{-2} d^{-1} (Moran et al., 2005). Values are mean (SE) for duplicate cores. Bottom row is mean (SE) of stations.

Station	C mineralized (TOU) *μmol C m^{-2} h^{-1}*	% of export production	C mineralized (denitrification) *μmol C m^{-2} h^{-1}*	% of export production
CBL11	193 (22)	35 (4)	69 (3)	12 (0.6)
CBL13	109 (8)	20 (1)	35 (5)	6 (0.9)
H17	–	–	–	–
H29	123 (23)	22 (4)	30 (5)	6 (0.8)
H33	315 (116)	57 (21)	54 (10)	10 (1.8)
Station mean (SE)	185 (47)	34 (9)	47 (9)	9 (2)

Figure 1

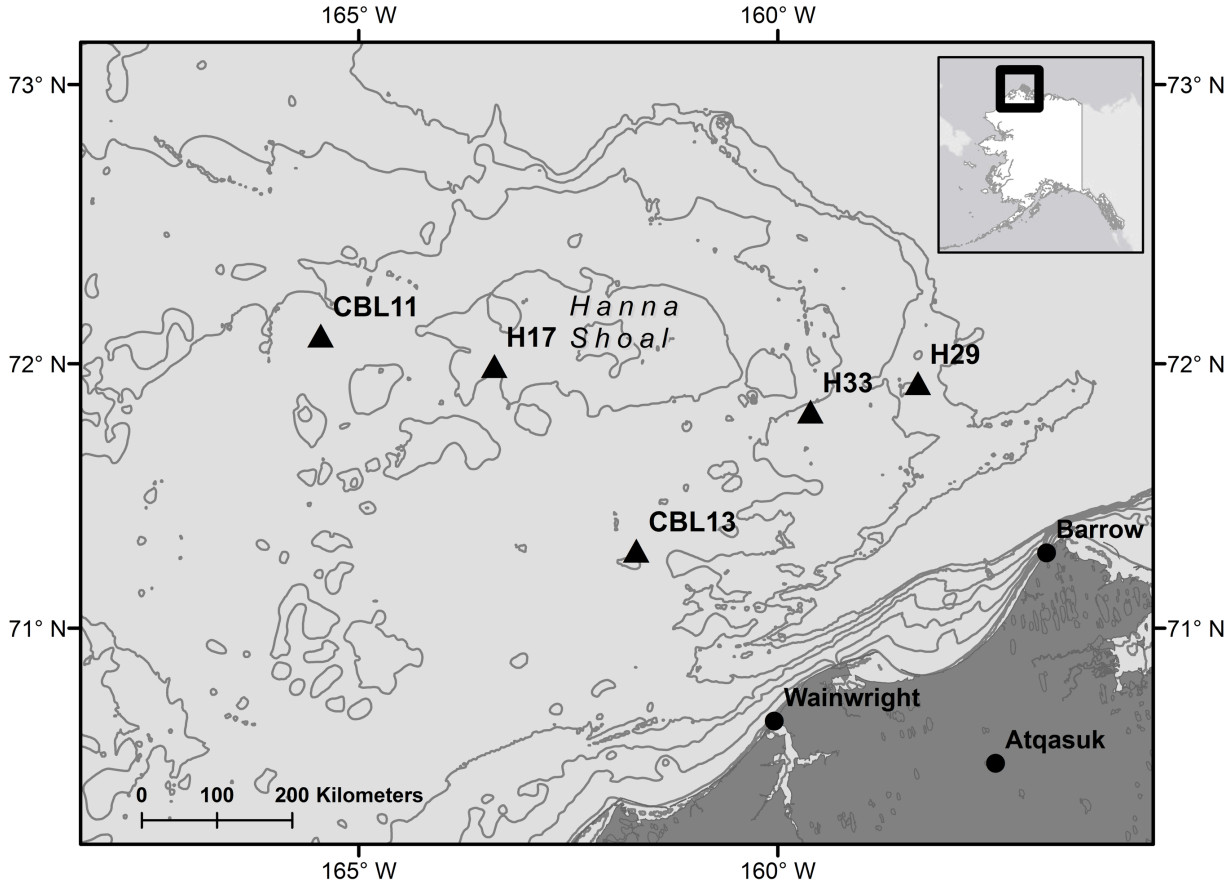
165° W
160° W
73° N
72° N
71° N
CBL11
Hanna
H17 Shoal
H29
H33
CBL13
Barrow
Wainwright
Atqasuk
0 100 200 Kilometers

Figure 2

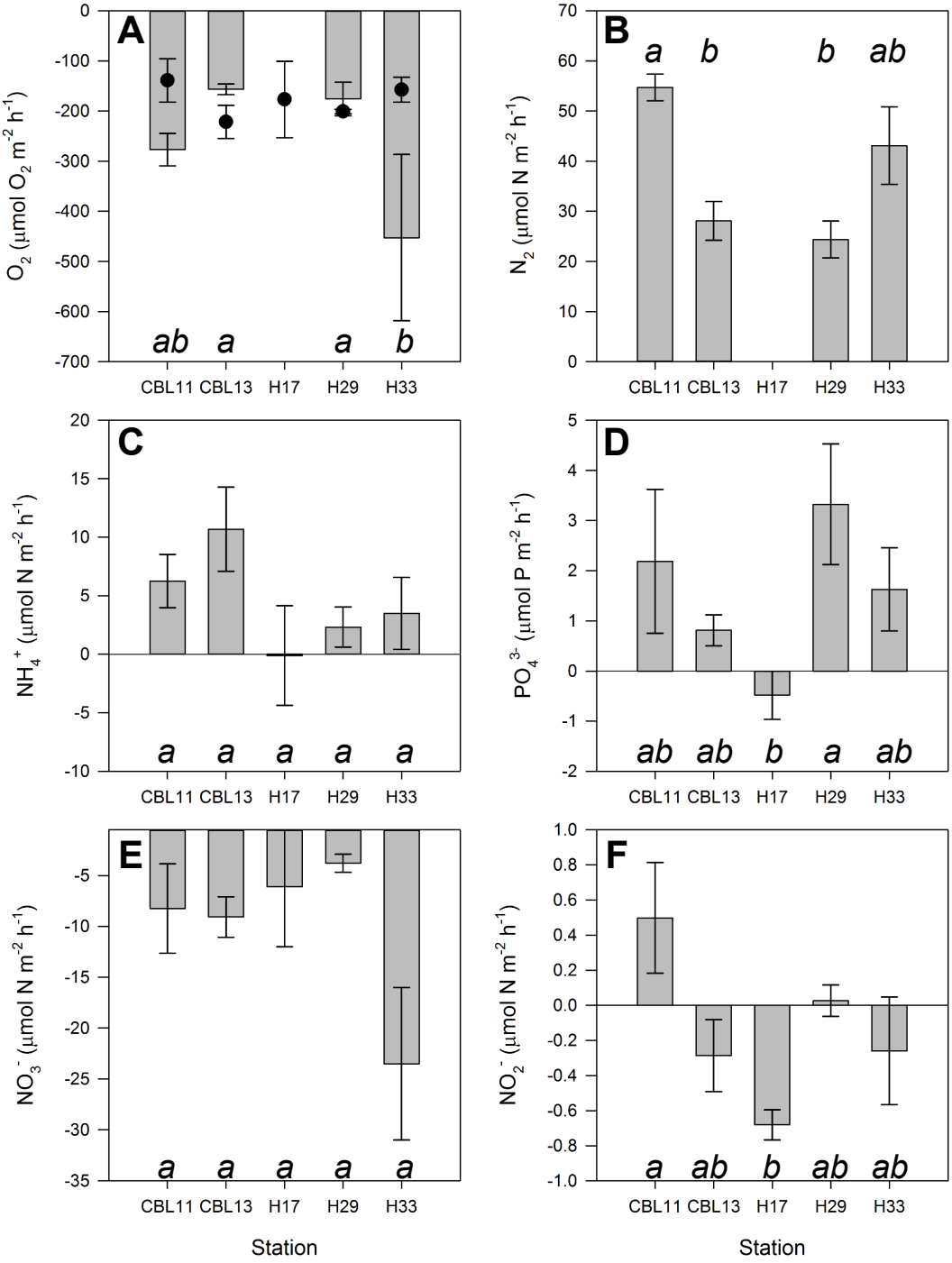
A
B
C
D
E
F
O_2 (µmol O_2 m^{-2} h^{-1})
N_2 (µmol N m^{-2} h^{-1})
NH_4^+ (µmol N m^{-2} h^{-1})
PO_4^{3-} (µmol P m^{-2} h^{-1})
NO_3^- (µmol N m^{-2} h^{-1})
NO_2^- (µmol N m^{-2} h^{-1})
ab a a b
a b b ab
a a a a a
ab ab b a ab
a a a a a
a ab b ab ab
CBL11 CBL13 H17 H29 H33
Station

Figure 3

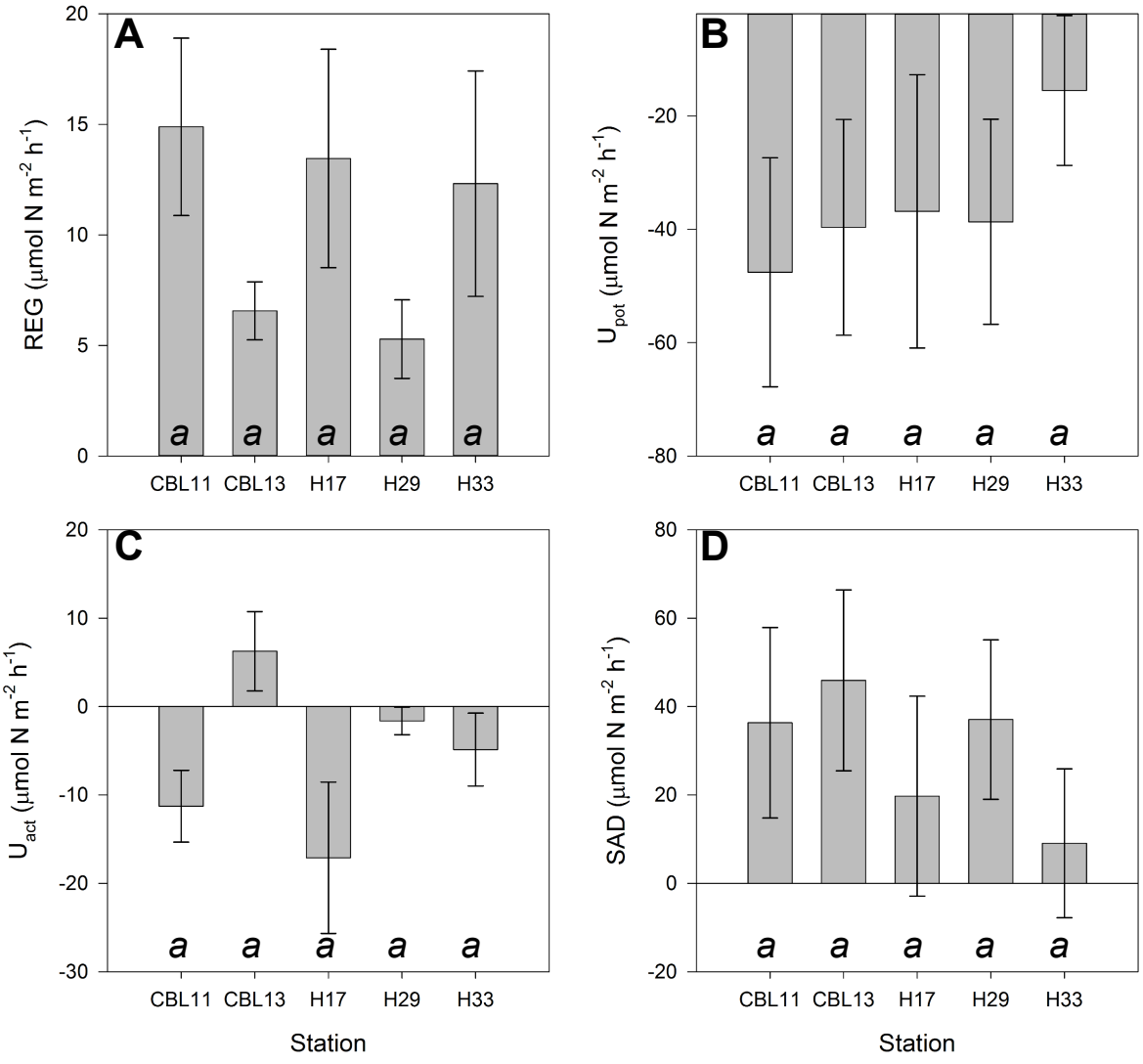
A
REG (µmol N m-2 h-1)
20
15
10
5
0
a a a a a
CBL11 CBL13 H17 H29 H33
B
Upot (µmol N m-2 h-1)
-20
-40
-60
-80
a a a a a
CBL11 CBL13 H17 H29 H33
C
Uact (µmol N m-2 h-1)
20
10
0
-10
-20
-30
a a a a a
CBL11 CBL13 H17 H29 H33
Station
D
SAD (µmol N m-2 h-1)
80
60
40
20
0
-20
a a a a a
CBL11 CBL13 H17 H29 H33
Station

Figure 4

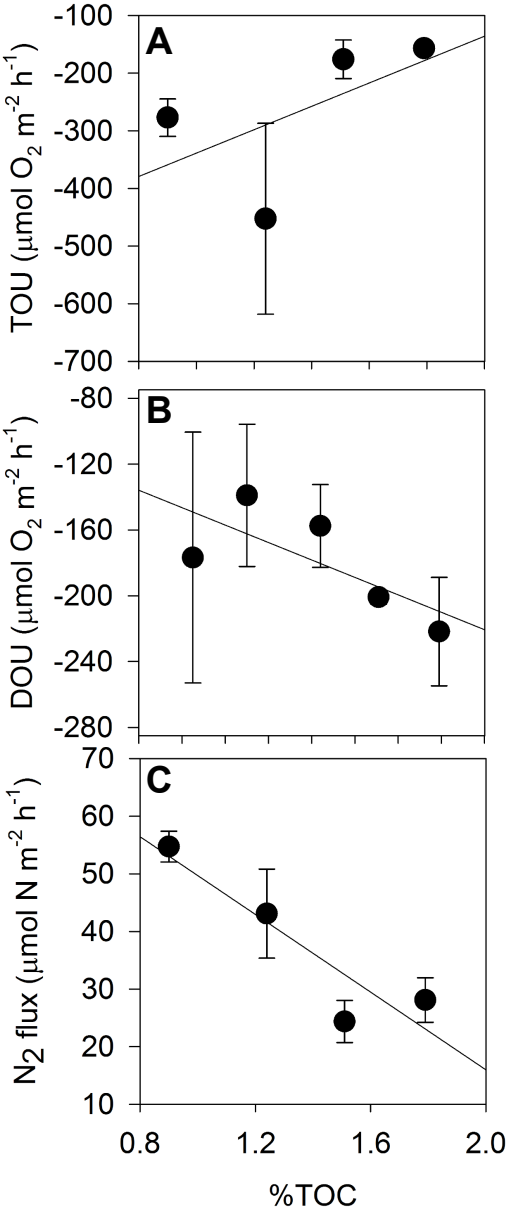
A
B
C
TOU (µmol O2 m-2 h-1)
DOU (µmol O2 m-2 h-1)
N2 flux (µmol N m-2 h-1)
-100
-200
-300
-400
-500
-600
-700
-80
-120
-160
-200
-240
-280
70
60
50
40
30
20
10
0.8
1.2
1.6
2.0
%TOC

Figure 5

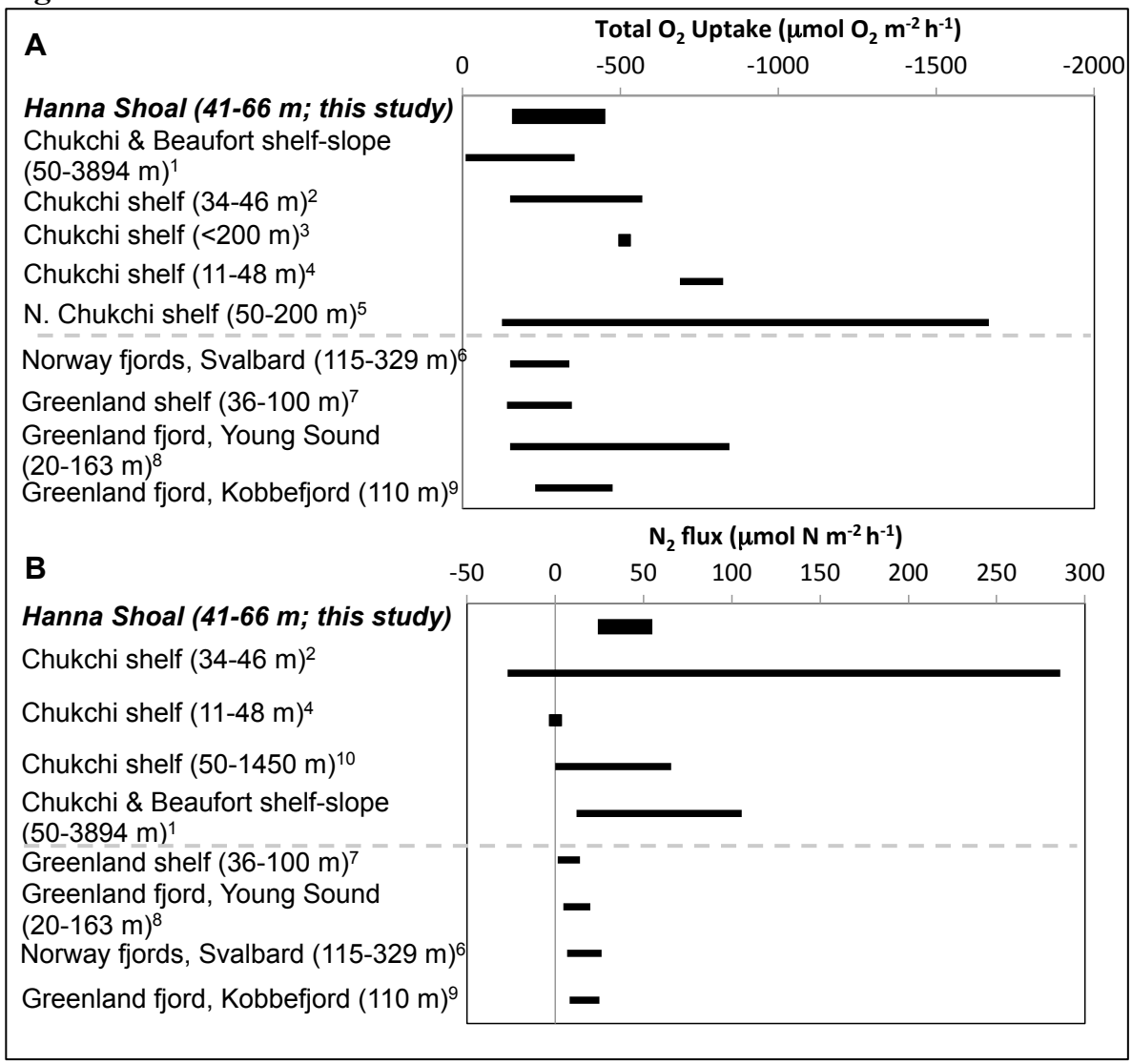
A
Total O_2 Uptake (μmol O_2 m^{-2} h^{-1})
0
-500
-1000
-1500
-2000
Hanna Shoal (41-66 m; this study)
Chukchi & Beaufort shelf-slope (50-3894 m)[1]
Chukchi shelf (34-46 m)[2]
Chukchi shelf (<200 m)[3]
Chukchi shelf (11-48 m)[4]
N. Chukchi shelf (50-200 m)[5]
Norway fjords, Svalbard (115-329 m)[6]
Greenland shelf (36-100 m)[7]
Greenland fjord, Young Sound (20-163 m)[8]
Greenland fjord, Kobbefjord (110 m)[9]
B
N_2 flux (μmol N m^{-2} h^{-1})
-50
0
50
100
150
200
250
300
Hanna Shoal (41-66 m; this study)
Chukchi shelf (34-46 m)[2]
Chukchi shelf (11-48 m)[4]
Chukchi shelf (50-1450 m)[10]
Chukchi & Beaufort shelf-slope (50-3894 m)[1]
Greenland shelf (36-100 m)[7]
Greenland fjord, Young Sound (20-163 m)[8]
Norway fjords, Svalbard (115-329 m)[6]
Greenland fjord, Kobbefjord (110 m)[9]

Figure 6

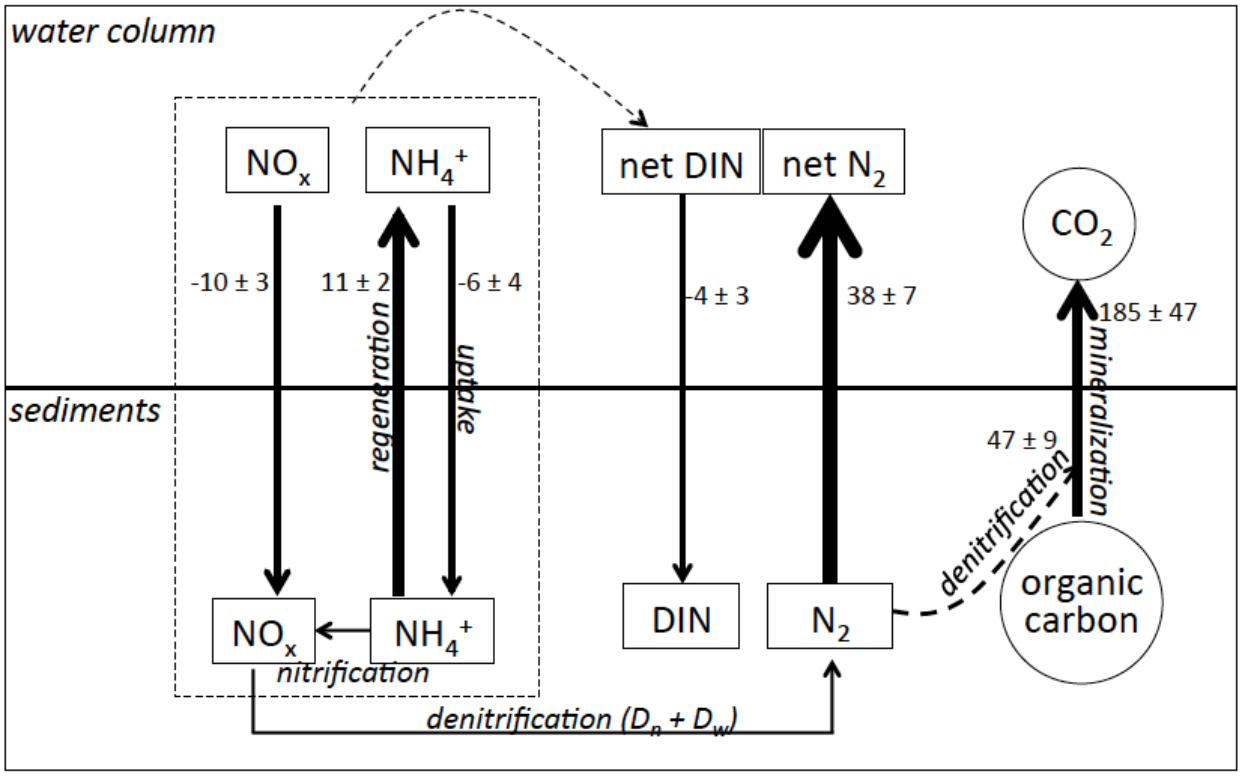
water column
sediments
NO$_x$
NH$_4^+$
net DIN
net N$_2$
CO$_2$
-10 ± 3
11 ± 2
-6 ± 4
-4 ± 3
38 ± 7
185 ± 47
regeneration
uptake
mineralization
47 ± 9
denitrification
organic carbon
NO$_x$
NH$_4^+$
DIN
N$_2$
nitrification
denitrification (D_n + D_w)